ACS OMEGA

http://pubs.acs.org/journal/acsodf

Article

Phase Behavior of Ternary Polymer Mixtures in a Common Solvent

Arjen Bot and Paul Venema*

Cite This: *ACS Omega* 2023, 8, 28387−28408

Read Online

ACCESS | Metrics & More | Article Recommendations | Supporting Information

ABSTRACT: The Edmond−Ogston model for phase separation is extended to ternary polymer mixtures in a common solvent (de facto a quaternary mixture). The model assumes a truncated virial expansion of the Helmholtz free energy up to the second-order terms in the concentration of the polymers, and the second virial coefficients (B_{11}, B_{22}, B_{33}, B_{12}, B_{13}, B_{23}) are the six parameters of the model. New results from this model are presented in relation to earlier work on binary mixtures: a necessary condition for the virial coefficients for the occurrence of phase separation in two or three phases, an analysis of the different regions of (local) thermodynamic instability using the Descartes sign rule, an expression for the critical curves, a relation between the tangents in points along the critical curve, a relation between the concentration of components in the different phases according to the so-called Lambert-W function, and a consistency check for the composition of coexisting phases in ternary mixtures. The obtained results are evaluated in the maximally symmetric version of the model, where (B_{11}, B_{22}, B_{33}) are equal and (B_{12}, B_{13}, B_{23}) are equal, which leads to two remarkable observations: the concentration range over which two phases are formed is relatively narrow; not all phase separation occurs within a Gibbs triangle, but also, "out-of-Gibbs-triangle" binodals are observed. These results lead to a deeper insight into the phase behavior of ternary mixtures and show promise as a stepping stone toward modeling phase separation in mixtures with many components.

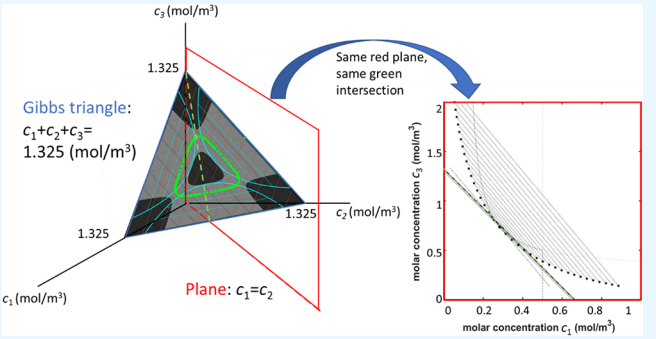

INTRODUCTION

Phase separation is a phenomenon where multiple components in solution do not fully mix at a molecular scale. It occurs when the concentrations of the components are too high to ignore their interactions, eventually leading to liquid−liquid phase separation. Phase separation has applications in fields as diverse as archaeology, forensics, hematology, wastewater treatment, food technology, and cell biology.[1−6] The present paper will specifically consider situations where the components are polymers, even though the formalism will be applicable more generally.

In previous work,[7−11] phase separation in binary polymer mixtures was investigated in terms of the mean-field Edmond−Ogston model,[12] which is based on a virial expansion of the Helmholtz free energy up to the second order in concentration. It should be stressed that "binary" refers here to the number of polymers involved and that these mixtures would be considered as ternary mixtures if the common solvent was counted as a component too. The Edmond−Ogston model allows one to make a fair prediction of the experimentally observed segregative phase behavior of a mixture while needing only three (positive) virial coefficients as input parameters in the case of a binary mixture. As part of that previous work, a number of analytical expressions were derived for binary mixtures, e.g., for the coordinates of the critical point. It was shown that larger sets of experimental binary phase diagrams with shared components can be used to determine the virial coefficients in a consistent way.[13]

Binary phase diagrams should be considered as an idealization of the real complex situation at hand, as most real-life mixtures contain multiple components and are polydisperse. It is therefore of interest to extend the Edmond−Ogston model to polydisperse, multicomponent mixtures. As a first step, the present paper aims to generalize this model to ternary mixtures. Historically, Edmond and Ogston themselves made the first attempt,[14] but without making general predictions on phase behavior. Ternary mixtures also provide a natural system to test the determination of virial coefficients from phase diagrams for mixtures with shared components.[13] In general, work on phase behavior of multicomponent polymer mixtures is limited. Mace et al. presented an experimentally obtained database for multicomponent systems ranging from two to five phases.[3] Phase separation of ternary mixtures without a common solvent was studied by Huang et al.[15] Zhou et al. investigated

Received: April 16, 2023
Accepted: June 30, 2023
Published: July 26, 2023

the kinetics of the phase separation for polymer/colloid mixtures in a common solvent.[16] Mao et al. calculated the phase behavior of multicomponent liquid mixtures.[17] Polydisperse systems were discussed by Warren,[18] Sear and Frenkel,[19] Sollich,[20] Edelman et al.,[21] and Sturtewagen and van der Linden.[22,23]

Here, the theory will be presented for systems with three components ($N = 3$) in a common solvent forming one, two, or three phases ($P = 1$, 2, or 3), where the common solvent is not explicitly counted as a component. It is noted that this makes these systems de facto quaternary mixtures. An explicit criterion is derived for the occurrence of phase separation in two or three phases in terms of the virial coefficients. Also, analytical expressions for the spinodal surfaces are obtained, and a simple relation for the critical curve in terms of the tangents along the critical curve is derived. Explicit expressions for binodal surfaces are obtained in some special cases. Several numerical results are included for the so-called (maximally) symmetric mixtures where (B_{11}, B_{22}, and B_{33}) are equal and (B_{12}, B_{13}, and B_{23}) are equal. A mapping is obtained between the parameters of the Edmond−Ogston and Flory−Huggins−de Gennes models for ternary mixtures in the limit of (maximally) symmetric mixtures. The line of thought is presented in the main text, and the mathematical details of the derivations are given in Appendices A.1-6.

METHODS: THEORY

Expressions for the Helmholtz Energy, Chemical Potentials, and Osmotic Pressure. The starting point for this work is an expression for the Helmholtz free energy F for a three-component mixture (not counting the solvent) where only terms up to the second order in concentration are taken into account

$$\frac{F}{RTV} = c_1\ln(c_1) + c_2\ln(c_2) + c_3\ln(c_3) + B_{11}c_1^2 + B_{22}c_2^2 + B_{33}c_3^2 + 2B_{12}c_1c_2 + 2B_{13}c_1c_3 + 2B_{23}c_2c_3 \quad (1)$$

with T (K) the absolute temperature, R (J/(K · mol)) the gas constant, V (m^3) the total volume of the system, c_i (mol/m^3) the concentration of polymer i ($i = 1$, 2, or 3) in molar units, B_{ii} (m^3/mol) the second virial coefficient of polymer i ($i = 1$, 2, or 3), and B_{ij} the second cross-virial coefficient for polymers i and j ($i,j = 1$, 2, or 3; $i \neq j$). The analysis is limited to phase separation where all second virial coefficients B_{ij} ($i,j = 1$, 2, or 3) are positive. The formal definition for the virial coefficients involves an averaging of the interaction potentials between the different components where the contributions of the solvent molecules are integrated out and can be found, e.g., in the work of McMillan and Mayer.[24] It should be noted that therefore, second virial coefficients in the Edmond−Ogston model include the interaction of the polymer with the solvent (which differs from, e.g., Flory−Huggins theory, where this interaction is captured in a separate parameter). From eq 1 expressions for the osmotic pressure Π and chemical potential μ_i of component i can be derived as

$$\frac{\Pi}{RT} = -\frac{1}{RT}\left(\frac{\partial F}{\partial V}\right)_{T,n_1,n_2,n_3} = c_1 + c_2 + c_3 + B_{11}{c_1}^2 + B_{22}{c_2}^2 + B_{33}{c_3}^2 + 2B_{12}c_1c_2 + 2B_{13}c_1c_3 + 2B_{23}c_2c_3 \quad (2)$$

$$\frac{\mu_1}{RT} = \frac{1}{RT}\left(\frac{\partial F}{\partial n_1}\right)_{T,V,n_2,n_3} = \ln c_1 + 2B_{11}c_1 + 2B_{12}c_2 + 2B_{13}c_3 + 1 \quad (3)$$

$$\frac{\mu_2}{RT} = \frac{1}{RT}\left(\frac{\partial F}{\partial n_2}\right)_{T,V,n_1,n_3} = \ln c_2 + 2B_{22}c_2 + 2B_{12}c_1 + 2B_{23}c_3 + 1 \quad (4)$$

$$\frac{\mu_3}{RT} = \frac{1}{RT}\left(\frac{\partial F}{\partial n_3}\right)_{T,V,n_1,n_2} = \ln c_3 + 2B_{33}c_3 + 2B_{13}c_1 + 2B_{23}c_2 + 1 \quad (5)$$

where n_i (mol) is the number of moles of component i and $c_i = n_i/V$ the molar concentration. Note that eq 2 is related to the expression for the chemical potential of the solvent, through the relation $\mu_s = -\upsilon_s\Pi$, with υ_s the partial volume of the solvent. These equations form the basis of the thermodynamic description of phase equilibria and can be used to describe one-phase, two-phase, and three-phase systems. If N is the number of components and P the number of phases, two cases are of particular interest here: two-phase ($N = 3$, $P = 2$) and three-phase ($N = 3$, $P = 3$) ternary systems.

Hessian Matrix M_1. To analyze the local stability of the mixture against phase separation, it is convenient to introduce the so-called Hessian matrix $\boldsymbol{M}_1$ with matrix elements $\boldsymbol{M}_1(i,j)$. The Hessian matrix characterizes the local curvature of the Helmholtz free energy surface. The matrix elements are defined as

$$\boldsymbol{M}_1(i,j) = \left(\frac{\partial}{\partial c_i}\left(\frac{\partial}{\partial c_j}\left(\frac{F}{RTV}\right)\right)_{T,V,c_{k\neq j}}\right)_{T,V,c_{k\neq i}} = \frac{\delta_{ij}}{c_i} + 2B_{ij} \quad (6)$$

where δ_{ij} corresponds to the Kronecker delta ($\delta_{ii} = 1$, $\delta_{ij} = 0$ for $i \neq j$). In the above equations, i, j, and $k = 1$, 2, or 3. Since the Helmholtz free energy F is a state variable, the Hessian matrix $\boldsymbol{M}_1$ fulfills the symmetry relation $\boldsymbol{M}_1(i,j) = \boldsymbol{M}_1(j,i)$ (i.e., the Maxwell relations). In matrix notation, $\boldsymbol{M}_1$ reads

$$\boldsymbol{M}_1 = \begin{pmatrix} \frac{1}{c_1} + 2B_{11} & 2B_{12} & 2B_{13} \\ 2B_{12} & \frac{1}{c_2} + 2B_{22} & 2B_{23} \\ 2B_{13} & 2B_{23} & \frac{1}{c_3} + 2B_{33} \end{pmatrix} \quad (7)$$

Since the matrix $\boldsymbol{M}_1$ reflects the local curvature of the free energy surface, it relates to the local stability against phase separation.

Stability Criteria. Since the matrix $\boldsymbol{M}_1$ is symmetric and all its elements are real, it can be diagonalized in terms of its eigenvalues and eigenvectors. Each of the three eigenvalues reflects the local curvature of the surface: positive eigenvalues indicate a convex curvature and negative eigenvalues indicate a concave curvature. Convex surfaces are associated with regions in the phase diagram that are locally stable against phase separation, and the opposite is valid for concave surfaces. The

https://doi.org/10.1021/acsomega.3c02604
ACS Omega 2023, 8, 28387−28408

eigenvalues λ and associated eigenvectors can be determined by the so-called characteristic equation

$$\mathrm{Det}(\boldsymbol{M_1} - \lambda \boldsymbol{I}) = 0 \tag{8}$$

where $\boldsymbol{I}$ represents the unit matrix. Furthermore, since matrix $\boldsymbol{M_1}$ is real and symmetric, it follows that $\mathrm{Det}(\boldsymbol{M_1}) = \lambda_1\lambda_2\lambda_3$, where λ_1, λ_2, and λ_3 are three real eigenvalues. In case all three eigenvalues are positive, the system is locally stable against concentration fluctuations, the system will not phase separate, and $\mathrm{Det}(\boldsymbol{M_1}) > 0$. However, the system can still be metastable against concentration fluctuations that are large enough. If one of the eigenvalues is negative, the system is unstable against concentration fluctuations and $\mathrm{Det}(\boldsymbol{M_1}) < 0$. If two of the eigenvalues are negative, the system is unstable against concentration fluctuations and $\mathrm{Det}(\boldsymbol{M_1}) > 0$. It will be shown later that for the present model, it is impossible to have three negative eigenvalues. The requirement from eq 8 in terms of λ is obtained as

$$\begin{aligned} &c_1c_2c_3\mathrm{Det}(\boldsymbol{M_1} - \lambda \boldsymbol{I}) \\ &= c_1c_2c_3\lambda^3 - \{(1 + 2B_{11}c_1)c_2c_3 + (1 + 2B_{22}c_2)c_1c_3 \\ &\quad + (1 + 2B_{33}c_3)c_2c_3\}\lambda^2 + \{(1 + 2B_{11}c_1) \\ &\quad (1 + 2B_{22}c_2)c_3 + (1 + 2B_{11}c_1)(1 + 2B_{33}c_3)c_2 \\ &\quad + (1 + 2B_{22}c_2)(1 + 2B_{33}c_3)c_1 - 4({B_{23}}^2 + {B_{13}}^2 \\ &\quad + {B_{12}}^2)c_1c_2c_3\}\lambda + 4{B_{23}}^2c_2c_3(1 + 2B_{11}c_1) \\ &\quad + 4{B_{13}}^2c_1c_3(1 + 2B_{22}c_2) + 4{B_{12}}^2c_1c_2(1 + 2B_{33}c_3) \\ &\quad - 16B_{12}B_{13}B_{23}c_1c_2c_3 - (1 + 2B_{11}c_1)(1 + 2B_{22}c_2) \\ &\quad (1 + 2B_{33}c_3) \\ &= 0 \end{aligned} \tag{9}$$

Using the sign rule of Descartes, it is possible to identify the maximum number of positive and negative roots for the characteristic polynomial (eq 9) for positive virial coefficients. It is noted, that since all roots are real, the maximum number of roots equals the actual number of roots. In Table 1 the

Table 1. The Number of Positive (+) and Negative (−) Roots for $a_3\lambda^3 + a_2\lambda^2 + a_1\lambda + a_0 = 0$ (Equation 9) According to the Descartes Sign Rule

sign a_3	+	+	+	+
sign a_2	−	−	−	−
sign a_1	+	+	−	−
sign a_0	+	−	+	−
number of sign changes	2	3	2	1
number of positive roots	2	3	2	1
number of negative roots	1	0	1	2

numbers of positive and negative roots are listed for the possible combinations of the signs of the coefficients of the characteristic polynomial. It is noted that this approach can be readily generalized for mixtures with more than three components since it is not needed to explicitly determine the roots of the characteristic equation to find the respective regions of instability.

When coefficients $a_0 < 0 \wedge a_1 > 0$, all three λ are positive, when $a_0 > 0$, there is one negative λ, and when $a_0 < 0 \wedge a_1 < 0$, there are two negative λ.

The requirement for $a_0 > 0$ (one negative λ) reads

$$\begin{aligned} a_0 \equiv\ & 4{B_{23}}^2c_2c_3(1 + 2B_{11}c_1) + 4{B_{13}}^2c_1c_3(1 + 2B_{22}c_2) \\ & + 4{B_{12}}^2c_1c_2(1 + 2B_{33}c_3) - 16B_{12}B_{13}B_{23}c_1c_2c_3 \\ & - (1 + 2B_{11}c_1)(1 + 2B_{22}c_2)(1 + 2B_{33}c_3) \\ >\ & 0 \end{aligned} \tag{10}$$

The two requirements that $a_0 < 0 \wedge a_1 < 0$ (two negative λ) read

$$\begin{aligned} a_0 \equiv\ & 4{B_{23}}^2c_2c_3(1 + 2B_{11}c_1) + 4{B_{13}}^2c_1c_3(1 + 2B_{22}c_2) \\ & + 4{B_{12}}^2c_1c_2(1 + 2B_{33}c_3) - 16B_{12}B_{13}B_{23}c_1c_2c_3 \\ & - (1 + 2B_{11}c_1)(1 + 2B_{22}c_2)(1 + 2B_{33}c_3) \\ <\ & 0 \end{aligned} \tag{11}$$

and

$$\begin{aligned} a_1 \equiv\ & (1 + 2B_{11}c_1)(1 + 2B_{22}c_2)c_3 + (1 + 2B_{11}c_1) \\ & (1 + 2B_{33}c_3)c_2 + (1 + 2B_{22}c_2)(1 + 2B_{33}c_3)c_1 \\ & - 4({B_{23}}^2 + {B_{13}}^2 + {B_{12}}^2)c_1c_2c_3 \\ <\ & 0 \end{aligned} \tag{12}$$

It is stressed that phase separation may still occur outside the unstable regions since there are metastable regions in the phase diagram. Such metastable regions are located between the so-called spinodal and binodal surfaces. The binodal surface will be discussed later but consists of all possible coexisting phases and can obtained by solving the coexistence equations (eqs 37−40). The spinodal surface separates the unstable and (meta-)stable regions in the phase diagram. In the unstable region, phase separation takes place spontaneously by spinodal decomposition, where concentration fluctuations grow unhindered. In the metastable region, there is a free energy barrier against phase separation, which takes place only when the concentration fluctuations are large enough, following a nucleation and growth mechanism.

Spinodal Surface. The spinodal surface can be calculated from $\mathrm{Det}\,\boldsymbol{M_1} = 0$ (i.e., eq 8 with $\lambda = 0$), which can be written as

$$\begin{aligned} c_1c_2c_3\mathrm{Det}\,\boldsymbol{M_1} =\ & (1 + 2B_{11}c_1)\{(1 + 2B_{22}c_2)(1 + 2B_{33}c_3) \\ & - 4{B_{23}}^2c_2c_3\} + (1 + 2B_{33}c_3) \\ & \{(1 + 2B_{11}c_1)(1 + 2B_{22}c_2) - 4{B_{12}}^2c_1c_2\} \\ & + (1 + 2B_{22}c_2)\{(1 + 2B_{11}c_1)(1 + 2B_{33}c_3) \\ & - 4{B_{13}}^2c_1c_3\} + 16B_{12}B_{23}B_{13}c_1c_2c_3 \\ & - 2(1 + 2B_{11}c_1)(1 + 2B_{22}c_2)(1 + 2B_{33}c_3) \end{aligned} \tag{13}$$

where it should be noted that all spinodals satisfy eq 13, but not all solutions to eq 13 are spinodals because solutions to eq 13 sometimes separate two unstable regions.[25] Note that the right-hand side of this expression is equal to the coefficient a_0 in eq 10 and reduces to the expression for the spinodal for a binary polymer mixture[7,8] when setting $c_3 = 0$ in eq 13

$$4(B_{11}B_{22} - {B_{12}}^2)c_1c_2 + 2B_{11}c_1 + 2B_{22}c_2 + 1 = 0 \tag{14}$$

and similar limits are obtained for $c_1 = 0$ or $c_2 = 0$. It can be shown that the points on the spinodal surface can be written in the form

https://doi.org/10.1021/acsomega.3c02604
ACS Omega 2023, 8, 28387−28408

$$(c_{1,sp}, c_{2,sp}, c_{3,sp}) = \left(\frac{1}{2(B_{12}S_{sp,21} + B_{13}S_{sp,31} - B_{11})}, \frac{1}{2(B_{12}S_{sp,12} + B_{23}S_{sp,32} - B_{22})}, \frac{1}{2(B_{13}S_{sp,13} + B_{23}S_{sp,23} - B_{33})} \right) \quad (15)$$

by substitution of eq 15 into eq 13. Note that it may be necessary to multiply the numerator and denominator by a factor $S_{sp,ji}$ if $S_{sp,ij}$ goes to infinity. The $S_{sp,ij}$ can be interpreted as minus the tangent to the spinodal surface parallel to the (c_i, c_j)-plane,[10] and the range of the $S_{sp,ij}$'s is determined by the requirement that the coordinates in eq 15 are all real and positive. Alternatively, eq 15 can be considered to be a parametrization of the spinodal surface in terms of the parameters $S_{sp,ij}$. There are only three independent values for $S_{sp,ij}$ since the following relations hold

$$S_{sp,ij} \equiv -\frac{1}{S_{sp,jk}S_{sp,ki}} \equiv \frac{1}{S_{sp,ji}} \quad (16)$$

with $k \neq i,j$ since the $S_{sp,ij}$'s are tangent to the spinodal surface, parallel to the (c_i, c_j)-plane. Equation 15 is a natural extension of the use of tangents to the spinodal in the case for binary mixtures (ref 10; eq 33 in combination with the procedure followed in Appendix III of that paper). Note that by definition, $S_{sp,ii} \equiv -1$.

Critical Curves. The critical points (sometimes also referred to as plait points) defining the critical curve can be calculated from the following two conditions.[26−29]

$$\text{Det}\, \boldsymbol{M_1} = 0 \quad (17)$$

$$\text{Det}\, \boldsymbol{M_2} = 0 \quad (18)$$

where the matrix $\boldsymbol{M_2}$ can be obtained by replacing any of the rows in matrix $\boldsymbol{M_1}$ by the row vector

$$\left[\frac{\partial}{\partial c_1}(\text{Det}\ \boldsymbol{M_1}) \quad \frac{\partial}{\partial c_2}(\text{Det}\, \boldsymbol{M_1}) \quad \frac{\partial}{\partial c_3}(\text{Det}\, \boldsymbol{M_1}) \right] \quad (19)$$

For example, the 3x3 matrix $\boldsymbol{M_2}$ in which the third row is substituted by eq 19 (referred to as $\boldsymbol{M_2'''}$) reads

$$\mathbf{M_2'''} = \begin{pmatrix} \frac{1}{c_1} + 2B_{11} & 2B_{12} & 2B_{13} \\ 2B_{12} & \frac{1}{c_2} + 2B_{22} & 2B_{23} \\ M_2'''(3,1) & M_2'''(3,2) & M_2'''(3,3) \end{pmatrix}$$

with $M_2'''(3,j) = \left\{ 4B_{pq}{}^2 - \Pi_{k=p,q}\left(\frac{1}{c_k} + 2B_{kk}\right) \right\} \frac{1}{c_j{}^2}$ with $p,q = 1,2,3$ but $p,q \neq j$. The explicit expressions for the three versions of the determinant of matrix $\boldsymbol{M_2}$ where different rows of matrix $\boldsymbol{M_1}$ are replaced are given by

$$\begin{aligned} c_1^2c_2^2c_3^2\text{Det}\boldsymbol{M_2'''} = {} & (\ 4B_{12}B_{13}c_1c_3 - 2B_{23}c_3(1 + 2B_{11}c_1)\ ) \\ & (4B_{13}{}^2c_1c_3 - (1 + 2B_{11}c_1)(1 + 2B_{33}c_3)) \\ & -\ (\ 4B_{12}{}^2c_1c_2 - (1 + 2B_{11}c_1) \\ & (1 + 2B_{22}c_2))(4B_{12}{}^2c_1c_2 - (1 + 2B_{11}c_1) \\ & (1 + 2B_{22}c_2)) + (\ 4B_{12}B_{23}c_2c_3 \\ & - 2B_{13}c_3(1 + 2B_{22}c_2)\ ) \\ & (4B_{23}{}^2c_2c_3 - (1 + 2B_{22}c_2)(1 + 2B_{33}c_3)) \end{aligned} \quad (20)$$

where $\text{Det}\boldsymbol{M_2'}$, $\text{Det}\boldsymbol{M_2''}$, and $\text{Det}\boldsymbol{M_2'''}$ refer to the matrices with substitution in the first, second, and third row, respectively (where expressions for $\text{Det}\boldsymbol{M_2'}$ and $\text{Det}\boldsymbol{M_2''}$ are given in Appendix A.2). These three determinants are not the same but identical under cyclic permutation of their indices. It is noteworthy that the determinants for the ternary polymer mixtures contain the expression for the spinodal for the binary polymer mixtures (cf. Figure 1 in ref 8).

It is convenient to introduce the orientation of the tangent plane to the spinodal surface in the critical points $(c_{1,c}, c_{2,c}, c_{3,c})$ in terms of the tangents $S_{c,21}$ and $S_{c,31}$ to the (c_1, c_2)-plane and (c_1, c_3)-plane, respectively.

The points on the critical curve must take the form of eq 15 since they need to fulfill eq 17 for the spinodal surface

$$(c_{1,c}, c_{2,c}, c_{3,c}) = \left(\frac{1}{2(B_{12}S_{c,21} + B_{13}S_{c,31} - B_{11})}, \frac{1}{2(B_{12}S_{c,12} + B_{23}S_{c,32} - B_{22})}, \frac{1}{2(B_{13}S_{c,13} + B_{23}S_{c,23} - B_{33})} \right) \quad (21)$$

The other requirement for points on the critical curve is given by eq 18 and can be expressed as (Appendix A.2)

$$\frac{S_{c,11}^3}{c_{1,c}^2} + \frac{S_{c,21}^3}{c_{2,c}^2} + \frac{S_{c,31}^3}{c_{3,c}^2} = 0 \quad (22)$$

By substituting eq 21 into eq 22 and using the equivalent of eq 16 for the relation between the $S_{c,ij}$'s, it is found that

$$\begin{aligned} & (B_{12}S_{c,21} + B_{13}S_{c,31} - B_{11})^2 - S_{c,21} \\ & \quad (B_{12} - B_{23}S_{c,31} - B_{22}S_{c,21})^2 - S_{c,31} \\ & \quad (B_{13} - B_{23}S_{c,21} - B_{33}S_{c,31})^2 \\ & = 0 \end{aligned} \quad (23)$$

Equations 22 and 23 are generalizations of eq 3 in ref 11.

Figure 1 shows possible combinations of $S_{sp,21}$ and $S_{sp,31}$ for an arbitrary set of virial coefficients. The black dotted regions correspond to combinations of tangents that give rise to physical solutions (i.e., positive concentrations) for the spinodal surface, using

$$B_{12}S_{sp,21} + B_{13}S_{sp,31} - B_{11} > 0 \quad (24)$$

$$B_{12}S_{sp,12} + B_{23}S_{sp,32} - B_{22} > 0 \quad (25)$$

$$B_{13}S_{sp,13} + B_{23}S_{sp,23} - B_{33} > 0 \quad (26)$$

https://doi.org/10.1021/acsomega.3c02604
ACS Omega 2023, 8, 28387−28408

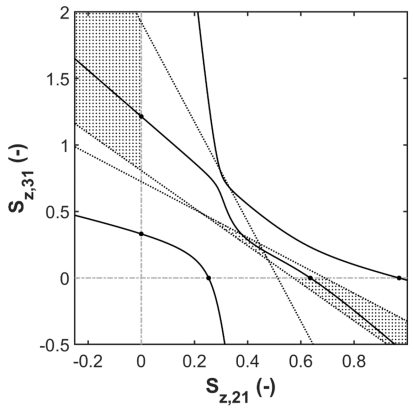

Figure 1. Regions indicating the physical relevant solutions for the spinodal and critical coordinates in terms of the tangents $S_{z,21}$ and $S_{z,31}$ (with z = *sp*, *c* or *m*, where *m* will be introduced later in this paper) and the relations between the critical tangents $S_{c,21}$ and $S_{c,31}$. (—): relation between $S_{c,21}$ and $S_{c,31}$ according to eq 22/23; (dotted region): physically relevant solutions, i.e., positive coordinates for the critical point or the spinodal surface (or the coordinates in eqs 46−48). The white regions indicate the parameter space where not all three critical point coordinates are positive, and where concentrations are unphysical; (....): bounds to the physically relevant regions representing $c_{1,c} \geq 0$ (eq 24), $c_{2,c} \geq 0$ (eq 25), and $c_{3,c} \geq 0$ (eq 26); (●) the (physical *and* unphysical) solutions for binary mixtures (for $S_{c,21}$ = 0.253,0.636,0.969 or $S_{c,31}$ = 0.331,1.21,6.00), that are located on the gray dash-dotted line that represent either $S_{c,31} = 0$ or $S_{c,21} = 0$. The plot was generated for an asymmetric ternary mixture with B_{11} = 1.43, B_{22} = 3.62, B_{33} = 0.92, B_{12} = 2.5, B_{13} = 1.77, B_{23} = 3.45 (m^3/mol).

where $S_{sp,32} \equiv -\frac{1}{S_{sp,21}S_{sp,13}} \equiv \frac{1}{S_{sp,23}}$. It can be easily shown that the boundary of the area with physical solutions (eqs 24−26) consists of lines. Figure 1 also shows the combinations of $S_{c,21}$ and $S_{c,31}$ that fulfill eq 23 (solid black curves). The parts where the black curves cross the black dotted areas correspond to physical solutions for the critical point (eq 21). Black solid circles indicate the (physical and unphysical) solutions for binary mixtures, when either $S_{c,21}$ or $S_{c,31}$ are zero and eq 22 reduces to eq 3 in ref 11. All the coordinates for the spinodal surface and critical curve can be obtained by substituting valid combinations of $S_{sp,21}$and $S_{sp,31}$ or $S_{c,21}$ and $S_{c,31}$ in eqs 15 and 21, respectively.

Necessary Conditions for the Virial Coefficients for Phase Formation. The criterion for the virial coefficients allowing for two negative eigenvalues at sufficiently high concentrations (i.e., c_1, c_2, $c_3 \to \infty$) can be derived from eqs 11 and 12, although it should be stressed that the metastable region may extend over a much wider range than the unstable region.[30] These two negative eigenvalues require that $a_0 < 0$ and $a_1 < 0$. The criterion for a_0 in eq 11 can be rewritten as

$$4{B_{23}}^2\left(\frac{1}{c_1} + 2B_{11}\right) + 4{B_{13}}^2\left(\frac{1}{c_2} + 2B_{22}\right) + 4{B_{12}}^2\left(\frac{1}{c_3} + 2B_{33}\right) - 16B_{12}B_{13}B_{23} - \left(\frac{1}{c_1} + 2B_{11}\right)\left(\frac{1}{c_2} + 2B_{22}\right)\left(\frac{1}{c_3} + 2B_{33}\right) < 0 \quad (27)$$

Taking the limit for infinitely high concentrations c_1, c_2, $c_3 \to \infty$ leads to

$${B_{23}}^2B_{11} + {B_{13}}^2B_{22} + {B_{12}}^2B_{33} - 2B_{12}B_{13}B_{23} - B_{11}B_{22}B_{33} < 0 \quad (28)$$

which can be rewritten as

$$\left(\frac{{B_{12}}^2}{B_{11}B_{22}} - 1\right) + \left(\frac{{B_{13}}^2}{B_{11}B_{33}} - 1\right) + \left(\frac{{B_{23}}^2}{B_{22}B_{33}} - 1\right) < 2\left(\frac{B_{12}}{\sqrt{B_{11}B_{22}}}\frac{B_{13}}{\sqrt{B_{11}B_{33}}}\frac{B_{23}}{\sqrt{B_{22}B_{33}}} - 1\right) \quad (29)$$

Analogously, the criterion for a_1 in eq 12 can be written as

$$\left\{\left(\frac{1}{c_1} + 2B_{11}\right)\left(\frac{1}{c_2} + 2B_{22}\right) - 4{B_{12}}^2\right\} + \left\{\left(\frac{1}{c_1} + 2B_{11}\right)\left(\frac{1}{c_3} + 2B_{33}\right) - 4{B_{13}}^2\right\} + \left\{\left(\frac{1}{c_2} + 2B_{22}\right)\left(\frac{1}{c_3} + 2B_{33}\right) - 4{B_{23}}^2\right\} = 0 \quad (30)$$

Taking the limit for infinitely high concentrations c_1, c_2, $c_3 \to \infty$ results in

$$\{{B_{12}}^2 - B_{11}B_{22}\} + \{{B_{13}}^2 - B_{11}B_{33}\} + \{{B_{23}}^2 - B_{22}B_{33}\} > 0 \quad (31)$$

In Appendix A.3, it is shown that criteria of eqs 29 and 31 imply that two negative eigenvalues can occur only if

$$\left(\frac{{B_{12}}^2}{B_{11}B_{22}} > 1\right) \wedge \left(\frac{{B_{13}}^2}{B_{11}B_{33}} > 1\right) \wedge \left(\frac{{B_{23}}^2}{B_{22}B_{33}} > 1\right) \quad (32)$$

i.e., each of the binary mixtures is able to phase separate individually (cf. refs 10 and 31).

The criterion for the virial coefficients allowing for one negative eigenvalue at sufficiently high concentrations (i.e., c_1, c_2, $c_3 \to \infty$) can be derived from eq 10, again stressing that the metastable region may extend over a much wider range than the unstable region. One or two of the criteria in eq 32 need to be satisfied simultaneously, but not all three

$$\left(\left(\frac{{B_{12}}^2}{B_{11}B_{22}} > 1\right) \vee \left(\frac{{B_{13}}^2}{B_{11}B_{33}} > 1\right) \vee \left(\frac{{B_{23}}^2}{B_{22}B_{33}} > 1\right)\right) \wedge \left(\neg\left(\left(\frac{{B_{12}}^2}{B_{11}B_{22}} > 1\right) \wedge \left(\frac{{B_{13}}^2}{B_{11}B_{33}} > 1\right) \wedge \left(\frac{{B_{23}}^2}{B_{22}B_{33}} > 1\right)\right)\right) \quad (33)$$

The formation of three phases is not predicted by having two negative eigenvalues (although two negative eigenvalues always coincide with the occurrence of three phases). Three phases are obtained if there are at least two (intersecting) binodals in the three-dimensional phase diagram. In that case, there are pairs of concentrations of coexisting phases on each of the two binodals, where one of the concentrations is shared. As a consequence, there are three coexisting phases in equilibrium if

https://doi.org/10.1021/acsomega.3c02604
ACS Omega 2023, 8, 28387−28408

at least two out of three components of the mixture satisfy the binary phase separation criterion:

$$\left(\left(\frac{B_{12}{}^2}{B_{11}B_{22}} > 1\right) \wedge \left(\frac{B_{13}{}^2}{B_{11}B_{33}} > 1\right) \wedge \left(\frac{B_{23}{}^2}{B_{22}B_{33}} > 1\right)\right) \vee \left(\left(\frac{B_{12}{}^2}{B_{11}B_{22}} > 1\right) \wedge \left(\frac{B_{13}{}^2}{B_{11}B_{33}} > 1\right)\right) \vee \left(\left(\frac{B_{12}{}^2}{B_{11}B_{22}} > 1\right) \wedge \left(\frac{B_{23}{}^2}{B_{22}B_{33}} > 1\right)\right) \vee \left(\left(\frac{B_{13}{}^2}{B_{11}B_{33}} > 1\right) \wedge \left(\frac{B_{23}{}^2}{B_{22}B_{33}} > 1\right)\right) \tag{34}$$

Coexistence Equations for $N = 3$ and $P = 2$. In the case of two phases, I and II, the osmotic pressure and all three chemical potentials need to be the same in each phase

$$\frac{\Pi^{I}}{RT} = \frac{\Pi^{II}}{RT} \tag{35}$$

$$\frac{\mu_i^{I}}{RT} = \frac{\mu_i^{II}}{RT} \tag{36}$$

with i = 1, 2, or 3. This gives in total 4 equations with 6 unknowns, and the requirement of mass balance adds another 3 equations with 1 unknown (the ratio of the two phase volumes), leading to a total of 7 equations with 7 unknowns. Using eqs 2−5, the explicit expressions for osmotic pressure and chemical potentials are

$$c_1^{I} + c_2^{I} + c_3^{I} + B_{11}c_1^{I2} + B_{22}c_2^{I2} + B_{33}c_3^{I2} + 2B_{12}c_1^{I}c_2^{I} + 2B_{13}c_1^{I}c_3^{I} + 2B_{23}c_2^{I}c_3^{I} = c_1^{II} + c_2^{II} + c_3^{II} + B_{11}c_1^{II2} + B_{22}c_2^{II2} + B_{33}c_3^{II2} + 2B_{12}c_1^{II}c_2^{II} + 2B_{13}c_1^{II}c_3^{II} + 2B_{23}c_2^{II}c_3^{II} \tag{37}$$

$$\ln(c_1^{I}) + 2B_{11}c_1^{I} + 2B_{12}c_2^{I} + 2B_{13}c_3^{I} + 1 = \ln(c_1^{II}) + 2B_{11}c_1^{II} + 2B_{12}c_2^{II} + 2B_{13}c_3^{II} + 1 \tag{38}$$

$$\ln(c_2^{I}) + 2B_{22}c_2^{I} + 2B_{12}c_1^{I} + 2B_{23}c_3^{I} + 1 = \ln(c_2^{II}) + 2B_{22}c_2^{II} + 2B_{12}c_1^{II} + 2B_{23}c_3^{II} + 1 \tag{39}$$

$$\ln(c_3^{I}) + 2B_{33}c_3^{I} + 2B_{13}c_1^{I} + 2B_{23}c_2^{I} + 1 = \ln(c_3^{II}) + 2B_{33}c_3^{II} + 2B_{13}c_1^{II} + 2B_{23}c_2^{II} + 1 \tag{40}$$

Solving the above equations will give all pairs (c_1^{I}, c_2^{I}, c_3^{I}) and (c_1^{II}, c_2^{II}, c_3^{II}) of coexisting phases that together define the binodal surface. Similar to an earlier approach,[10] it is convenient to introduce the following definitions for the minus the slope of the tie-lines

$$S_{m,ij} \equiv -\frac{c_i^{II} - c_i^{I}}{c_j^{II} - c_j^{I}} = -\frac{1}{S_{m,jk}S_{m,ki}} \equiv \frac{1}{S_{m,ji}} \tag{41}$$

with $k \neq i,j$, and c_i^{I} and c_i^{II} represent the concentration of component i in coexisting phases and I and II. Because of $S_{m,ii} \equiv -1$ and eq 41, there are only two independent $S_{m,ij}$. Substituting the above expressions into the coexistence equations (eqs 37−40) results in

$$(S_{m,21}B_{12} + S_{m,31}B_{13} - B_{11})(c_1^{I} + c_1^{II}) = +S_{m,21}(S_{m,12}B_{12} + S_{m,32}B_{23} - B_{22})(c_2^{I} + c_2^{II}) + S_{m,31}(S_{m,13}B_{13} + S_{m,23}B_{23} - B_{33})(c_3^{I} + c_3^{II}) + (1 - S_{m,21} - S_{m,31}) \tag{42}$$

$$\ln(c_1^{I}) + 2(B_{11} - B_{12}S_{m,21} - B_{13}S_{m,31})c_1^{I} = \ln(c_1^{II}) + 2(B_{11} - B_{12}S_{m,21} - B_{13}S_{m,31})c_1^{II} \tag{43}$$

$$\ln(c_2^{I}) + 2(B_{22} - B_{12}S_{m,12} - B_{23}S_{m,32})c_2^{I} = \ln(c_2^{II}) + 2(B_{22} - B_{12}S_{m,12} - B_{23}S_{m,32})c_2^{II} \tag{44}$$

$$\ln(c_3^{I}) + 2(B_{33} - B_{13}S_{m,13} - B_{23}S_{m,23})c_3^{I} = \ln(c_3^{II}) + 2(B_{33} - B_{13}S_{m,13} - B_{23}S_{m,23})c_3^{II} \tag{45}$$

Defining the auxiliary constants $c_{i,s}$ (with i = 1, 2, or 3) as

$$c_{1,s} = \frac{1}{2(B_{12}S_{m,21} + B_{13}S_{m,31} - B_{11})} \tag{46}$$

$$c_{2,s} = \frac{1}{2(B_{12}S_{m,12} + B_{23}S_{m,32} - B_{22})} \tag{47}$$

$$c_{3,s} = \frac{1}{2(B_{13}S_{m,13} + B_{23}S_{m,23} - B_{33})} \tag{48}$$

(again noting that it may be necessary to multiply the numerator and denominator by a factor $S_{m,ji}$ if $S_{m,ij}$ goes to infinity). The structure of eqs 46−47 is the same as eqs 15 and 21. This allows rewriting eq 42 as

$$\left(\frac{c_1^{I}}{c_{1,s}} - 1\right) + \left(\frac{c_1^{II}}{c_{1,s}} - 1\right) = S_{m,21}\left(\left(\frac{c_2^{I}}{c_{2,s}} - 1\right) + \left(\frac{c_2^{II}}{c_{2,s}} - 1\right)\right) + S_{m,31}\left(\left(\frac{c_3^{I}}{c_{3,s}} - 1\right) + \left(\frac{c_3^{II}}{c_{3,s}} - 1\right)\right) \tag{49}$$

and eqs 43−45 as

$$\ln\left(\frac{c_i^{I}}{c_{i,s}}\right) - \frac{c_i^{I}}{c_{i,s}} = \ln\left(\frac{c_i^{II}}{c_{i,s}}\right) - \frac{c_i^{II}}{c_{i,s}} \tag{50}$$

(i = 1, 2, or 3), which have the so-called Lambert-W function as solutions.[8,10,32] This expression links the concentration of each individual component in phase I to that in phase II. Generally, the concentrations can be on the same branch of the Lambert-W function (i.e., the component is evenly distributed over both phases), or they can be on separate branches (i.e., the component has a high concentration in one phase and a low concentration in the other). The $c_{i,s}$ should be positive to warrant real values in eq 50, setting a range for $S_{m,ij}$ that is identical to the range for $S_{sp,ij}$ in Figure 1. To find additional conditions needed to calculate the coexisting phases, eq 41 can be rewritten as

https://doi.org/10.1021/acsomega.3c02604
ACS Omega 2023, 8, 28387−28408

$$\left(\frac{c_i^{\mathrm{I}}}{c_{i,s}} - 1\right) - \left(\frac{c_i^{\mathrm{II}}}{c_{i,s}} - 1\right) = -S_{m,ij}\frac{c_{j,s}}{c_{i,s}}\left(\left(\frac{c_j^{\mathrm{I}}}{c_{j,s}} - 1\right) - \left(\frac{c_j^{\mathrm{II}}}{c_{j,s}} - 1\right)\right) \quad (51)$$

(i,j = 1, 2, or 3; $i \neq j$) and can be combined with eq 49. After some rearrangement, eqs 49 and 51 can be combined in matrix notation

$$\begin{pmatrix} \frac{c_1^{\mathrm{I}}}{c_{1,s}} - 1 \\ \frac{c_2^{\mathrm{I}}}{c_{2,s}} - 1 \\ \frac{c_3^{\mathrm{I}}}{c_{3,s}} - 1 \end{pmatrix} = \begin{pmatrix} \frac{\left(-\frac{1}{c_{1,s}} + \frac{S_{m,21}^2}{c_{2,s}} + \frac{S_{m,31}^2}{c_{3,s}}\right)}{\left(\frac{1}{c_{1,s}} + \frac{S_{m,21}^2}{c_{2,s}} + \frac{S_{m,31}^2}{c_{3,s}}\right)} & \frac{2S_{m,21}/c_{1,s}}{\left(\frac{1}{c_{1,s}} + \frac{S_{m,21}^2}{c_{2,s}} + \frac{S_{m,31}^2}{c_{3,s}}\right)} & \frac{2S_{m,31}/c_{1,s}}{\left(\frac{1}{c_{1,s}} + \frac{S_{m,21}^2}{c_{2,s}} + \frac{S_{m,31}^2}{c_{3,s}}\right)} \\ \frac{2S_{m,21}/c_{2,s}}{\left(\frac{1}{c_{1,s}} + \frac{S_{m,21}^2}{c_{2,s}} + \frac{S_{m,31}^2}{c_{3,s}}\right)} & \frac{\left(\frac{1}{c_{1,s}} - \frac{S_{m,21}^2}{c_{2,s}} + \frac{S_{m,31}^2}{c_{3,s}}\right)}{\left(\frac{1}{c_{1,s}} + \frac{S_{m,21}^2}{c_{2,s}} + \frac{S_{m,31}^2}{c_{3,s}}\right)} & \frac{-2S_{m,21}S_{m,31}/c_{2,s}}{\left(\frac{1}{c_{1,s}} + \frac{S_{m,21}^2}{c_{2,s}} + \frac{S_{m,31}^2}{c_{3,s}}\right)} \\ \frac{2S_{m,31}/c_{3,s}}{\left(\frac{1}{c_{1,s}} + \frac{S_{m,21}^2}{c_{2,s}} + \frac{S_{m,31}^2}{c_{3,s}}\right)} & \frac{-2S_{m,21}S_{m,31}/c_{3,s}}{\left(\frac{1}{c_{1,s}} + \frac{S_{m,21}^2}{c_{2,s}} + \frac{S_{m,31}^2}{c_{3,s}}\right)} & \frac{\left(\frac{1}{c_{1,s}} + \frac{S_{m,21}^2}{c_{2,s}} - \frac{S_{m,31}^2}{c_{3,s}}\right)}{\left(\frac{1}{c_{1,s}} + \frac{S_{m,21}^2}{c_{2,s}} + \frac{S_{m,31}^2}{c_{3,s}}\right)} \end{pmatrix} \begin{pmatrix} \frac{c_1^{\mathrm{II}}}{c_{1,s}} - 1 \\ \frac{c_2^{\mathrm{II}}}{c_{2,s}} - 1 \\ \frac{c_3^{\mathrm{II}}}{c_{3,s}} - 1 \end{pmatrix} \quad (52)$$

From eq 50 it follows that all the column vectors in eq 50 can be expressed in terms of Lambert-W functions of the concentrations in phase I (cf. eq 52 for binary mixtures in ref 10). This implies that instead of six concentration coordinates, there are only three of them in this problem.

Coexistence Equations for $N = 3$ and $P = 3$. In the case of three phases, I, II, and III, the osmotic pressure and all three chemical potentials need to be the same in each phase.

$$\frac{\Pi^{\mathrm{I}}}{RT} = \frac{\Pi^{\mathrm{II}}}{RT} = \frac{\Pi^{\mathrm{III}}}{RT} \quad (53)$$

$$\frac{\mu_i^{\mathrm{I}}}{RT} = \frac{\mu_i^{\mathrm{II}}}{RT} = \frac{\mu_i^{\mathrm{III}}}{RT} \quad (54)$$

with i = 1, 2, or 3. This gives in total 8 equations with 9 unknowns, which are similar in structure to eqs 37−40 (adding the equations for phase III). The requirement of mass balance adds another 3 equations with 2 unknowns (the ratio of the two phase volumes), leading to a total of 11 equations with 11 unknowns. Solving the above equations will give all triplets (c_1^{I}, c_2^{I}, c_3^{I}), (c_1^{II}, c_2^{II}, c_3^{II}), and (c_1^{III}, c_2^{III}, c_3^{III}) of coexisting phases that together define the binodal surface. The coexistence equations to be solved are in principle similar to eq 52, but with a second matrix to relate the concentrations in phase I to those in phase III. The increased number of phases makes this calculation numerically more challenging.

However, for large concentrations, the problem simplifies again, and for the remainder of this paragraph, we limit ourselves to this case. For binary mixtures composed of components 1 and 2, it was found that the slope $S_{\infty,21}$ of the tie-lines approaches $-\sqrt{B_{11}/B_{22}}$.[10] For ternary mixtures, similar expressions hold for $S_{\infty,31}$ and $S_{\infty,23}$. If three phases are formed, the coexisting phases are positioned in a plane. At large concentrations, this plane extends to the $c_i = 0$ (i = 1, 2, or 3) axes, and therefore, the slopes in these intersections need to be identical to those in the binary planes. From these requirements, one can conclude that the three phases can be found in the plane

$$\sqrt{B_{11}}c_1 + \sqrt{B_{22}}c_2 + \sqrt{B_{33}}c_3 = c_0 \quad (55)$$

with the parameter $c_0 \gg 0$ (mol$^{1/2}$/m$^{1/2}$). It is noted that this expression does not contain the cross-virial coefficients, as was to be expected because three phases consist of essentially pure components 1, 2, or 3 in this limit. Furthermore, this plane has the normal vector ($\sqrt{B_{11}}$, $\sqrt{B_{22}}$, $\sqrt{B_{33}}$), which differs from the normal vector (1, 1, 1) of the Gibbs triangle. This illustrates that representation in terms of Gibbs triangles is optimal only in the case of symmetric mixtures. Equation 55 is strictly valid only for large concentrations, where c_1, c_2, $c_3 \to \infty$, but is expected to be a reasonable approximation also at lower concentrations (cf. eq 66 in ref 10).

Consistency Check for Coexisting Phases in Ternary Mixtures. Following a similar approach as in previous work on binary mixtures,[11] it can be shown that the coexistence equations can be simply combined in expressions that solely depend on the concentrations of the coexisting phases and that do not contain the virial coefficients anymore (see Appendix A.6). For case $N = 3$, $P = 2$

$$(c_1^{\mathrm{I}} - c_1^{\mathrm{II}}) + (c_2^{\mathrm{I}} - c_2^{\mathrm{II}}) + (c_3^{\mathrm{I}} - c_3^{\mathrm{II}}) + \frac{1}{2}(c_1^{\mathrm{I}} + c_1^{\mathrm{II}})\ln\left(\frac{c_1^{\mathrm{II}}}{c_1^{\mathrm{I}}}\right) + \frac{1}{2}(c_2^{\mathrm{I}} + c_2^{\mathrm{II}})\ln\left(\frac{c_2^{\mathrm{II}}}{c_2^{\mathrm{I}}}\right) + \frac{1}{2}(c_3^{\mathrm{I}} + c_3^{\mathrm{II}})\ln\left(\frac{c_3^{\mathrm{II}}}{c_3^{\mathrm{I}}}\right) = 0 \quad (56)$$

and for case $N = 3$, $P = 3$

$$(c_1^{\mathrm{I}} - c_1^{\mathrm{II}}) + (c_2^{\mathrm{I}} - c_2^{\mathrm{II}}) + (c_3^{\mathrm{I}} - c_3^{\mathrm{II}}) + \frac{1}{2}(c_1^{\mathrm{I}} + c_1^{\mathrm{II}})\ln\left(\frac{c_1^{\mathrm{II}}}{c_1^{\mathrm{I}}}\right) + \frac{1}{2}(c_2^{\mathrm{I}} + c_2^{\mathrm{II}})\ln\left(\frac{c_2^{\mathrm{II}}}{c_2^{\mathrm{I}}}\right) + \frac{1}{2}(c_3^{\mathrm{I}} + c_3^{\mathrm{II}})\ln\left(\frac{c_3^{\mathrm{II}}}{c_3^{\mathrm{I}}}\right) = 0 \quad (57)$$

https://doi.org/10.1021/acsomega.3c02604
ACS Omega 2023, 8, 28387−28408

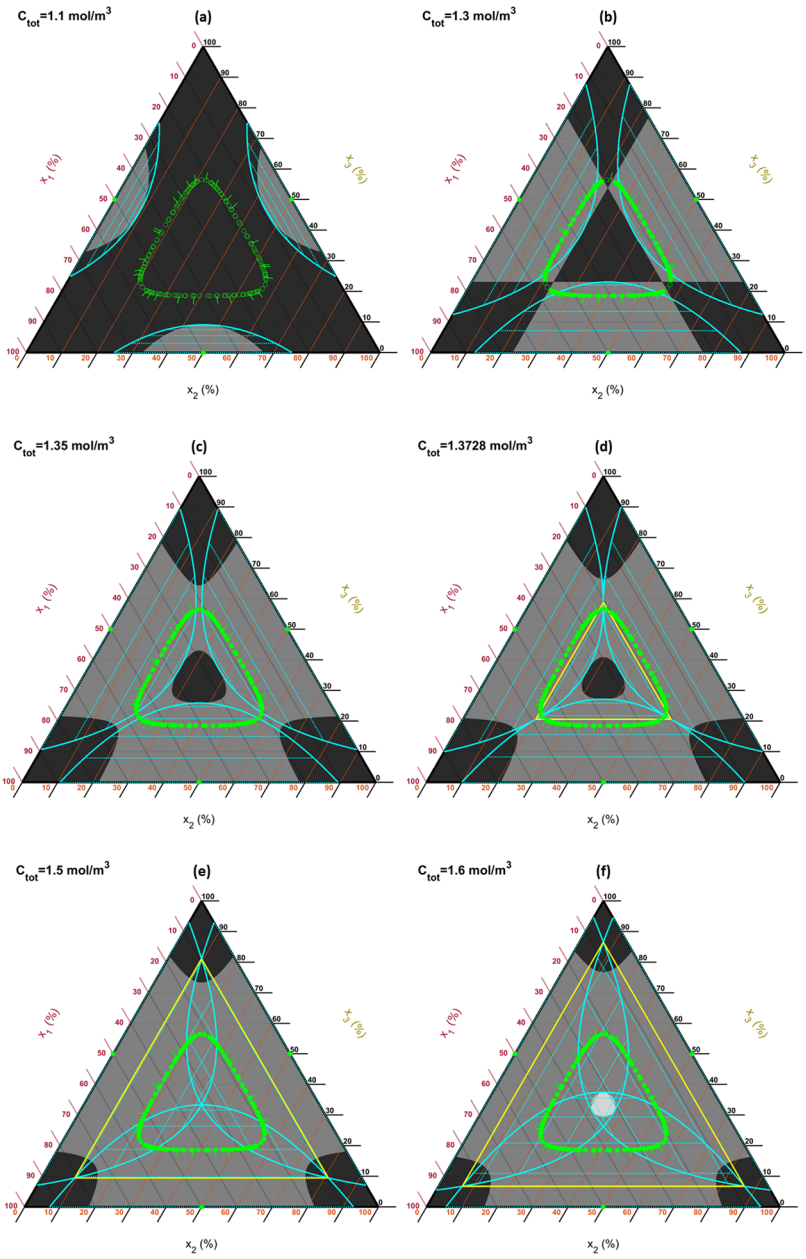

Figure 2. Examples of phase diagrams for c_{tot} = 1.1, 1.3, 1.35, 1.3728..., 1.5 and 1.6 mol/m^3 for the symmetric ternary mixture with B = 1 m^3/mol, C = 2 m^3/mol. At c_{tot} = 1.1 mol/m^3, the binodal for phase separation for binary mixtures starts to extend in the three-component region, but the three regions are still quite distinct. At c_{tot} = 1.3 mol/m^3, the spinodal curves separating the regions with zero and one negative eigenvalues are lines. The graph also shows the critical curve, where open green circles indicate critical points above the plane of constant c_{tot}, and solid green circles critical points below the plane of constant c_{tot} (the short green solid lines indicate the projection of the tangent to the critical surface to the Gibbs triangle according to Appendix A.5). At c_{tot} = 1.35 mol/m^3, the dark gray region becomes continuous. At c_{tot} = 1.3728... mol/m^3, the binodals touch and a three-phase equilibrium appears. At c_{tot} = 1.5 mol/m^3, the tops of the binodals meet in the center of the triangle and a minimum in the free energy start to develop near to the vertices leading to a three-phase equilibrium. At c_{tot} = 1.6 mol/m^3, the overlapping binodals give rise to a region with two negative eigenvalues. Yellow lines: triangle with three phases in equilibrium; Cyan solid lines: binodals; Cyan dotted lines: tie-lines; Light gray: two negative eigenvalues; Dark gray: one negative eigenvalue; Black region: zero negative eigenvalues. Note that a more extensive sequence of phase diagrams as a function of c_{tot} is available in the Supporting Information, Figures S3-S22.

$$(c_1^{\mathrm{I}} - c_1^{\mathrm{III}}) + (c_2^{\mathrm{I}} - c_2^{\mathrm{III}}) + (c_3^{\mathrm{I}} - c_3^{\mathrm{III}}) + \frac{1}{2}(c_1^{\mathrm{I}} + c_1^{\mathrm{III}}) \ln\left(\frac{c_1^{\mathrm{III}}}{c_1^{\mathrm{I}}}\right) + \frac{1}{2}(c_2^{\mathrm{I}} + c_2^{\mathrm{III}}) \ln\left(\frac{c_2^{\mathrm{III}}}{c_2^{\mathrm{I}}}\right) + \frac{1}{2}(c_3^{\mathrm{I}} + c_3^{\mathrm{III}}) \ln\left(\frac{c_3^{\mathrm{III}}}{c_3^{\mathrm{I}}}\right) = 0 \quad (58)$$

The above equation can replace any of the three coexistence equations without affecting the solutions. As such, it is a necessary but insufficient condition to determine the coexisting phases: all solutions to the coexistence equation fulfill eqs 56 (P = 2) or 57 and 58 (P = 3) but not the other way around. Even stronger, a combination of (c_1^{I}, c_2^{I}, c_3^{I}, c_1^{II}, c_2^{II}, c_3^{II}) that does not fulfill eq 56 for P = 2 or (c_1^{I}, c_2^{I}, c_3^{I}, c_1^{II}, c_2^{II}, c_3^{II}, c_1^{III}, c_2^{III}, c_3^{III}) that does not fullfil eqs 57 and 58 for P = 3 will not be a solution to

https://doi.org/10.1021/acsomega.3c02604
ACS Omega 2023, 8, 28387−28408

the coexistence equations for any combination of virial coefficients.

RESULTS: EXAMPLE FOR THE (MAXIMALLY) SYMMETRIC TERNARY MIXTURE ($B = B_{11} = B_{22} = B_{33}$; $C = B_{12} = B_{13} = B_{23}$)

The starting point for this discussion is the simplest condition for the symmetric ternary mixture, in which $B = B_{11} = B_{22} = B_{33}$ and $C = B_{12} = B_{13} = B_{23}$. The features of the ternary phase diagram will be discussed as a function of increasing total concentration. The discussion here will focus mainly on the physical aspects of the phase diagram, whereas the technical aspects of calculating the solutions will be dealt with in the Appendices.

The solutions to the coexisting equations for the symmetric ternary mixture have three symmetry planes, $c_i = c_j$ (i,j = 1, 2, or 3, with $i \neq j$). It is noted that the coexistence equations (eqs 35−38) for (in-Gibbs-triangle) maximally symmetric mixtures can be written in terms of $(C - B)c_i$ (see Appendix A.4).

In order to represent the three-dimensional (c_1, c_2, c_3) phase diagram in two dimensions, the phase diagrams for these symmetric mixtures will be mostly represented using the so-called Gibbs triangles[33] (and the plane in which the Gibbs triangles lie will be referred to as "in-Gibbs-triangle" here). These are cross sections of the three-dimensional phase diagram with the plane

$$c_{tot} = c_1 + c_2 + c_3 \tag{59}$$

with the total molar concentration c_{tot} acting as a parameter. Next x_i for i = 1, 2, or 3 can be defined as the molar fraction of each component

$$x_i = \frac{c_i}{c_{tot}} \tag{60}$$

The variables x_i are used to plot the Gibbs triangles at a fixed c_{tot}. Due to the symmetry of the mathematical problem, the phase diagram presented in the Gibbs triangles should be invariant under a $2\pi/3$ rotation. Figure 2 shows the phase diagram for different c_{tot} for B = 1 m^3/mol and C = 2 m^3/mol. Figure 2 is also available in the form of a short movie in the Supporting Information, featuring much smaller steps in concentration c_{tot}.

One-Phase Region. At concentrations $c_{tot} < \frac{1}{C-B}$, all components are miscible because for the binary symmetric mixture, any plane with $c_{tot} < \frac{1}{C-B}$ will lay below any of the three critical points, e.g., $\left(\frac{1}{2(C-B)}, \frac{1}{2(C-B)}, 0\right)$ (cf. refs 8 and 10. The $c_i = 0$ planes correspond to the sides of the Gibbs triangle. At c_{tot}=1 mol/m^3, where the critical points for the binary mixture just appear as indicated by the solid green circles in the middle of the sides of the Gibbs triangle (see Supporting Information, Figure S4). The open green circles will be discussed later. All eigenvalues $\lambda > 0$, represented by the black background, correspond to a region that is stable or metastable against concentration fluctuations. In this particular case, the black region in the Gibbs triangle refers to a stable region because the binodal was determined explicitly.

Two-Phase Region. For $\frac{1}{C-B} < c_{tot} < \frac{3B+5C}{4C^2-2B(B+C)}$ (see Appendix A.4 for the explanation of the upper limit), the two-phase regions are bound by three binodals that develop as the semimoonlike features from the sides of the triangle (cf. refs 15 and 34), and the black region is continuous (see Figure 2a for c_{tot}= 1.1 mol/m^3 and the Supporting Information for some additional c_{tot} values, Figures S5−S9). The three binodals lay in the Gibbs triangle, where c_{tot} is constant, and were calculated analytically (see Appendix A.4) and confirmed by solving eqs 37−40 numerically. It was found that for each of these binodals, one of the three components is evenly distributed over both phases, which is also reflected in eqs 95 and 96 in Appendix A.4. The tops of the three binodals in Figure 2a move toward the center of the Gibbs triangle with increasing c_{tot}. The tie-lines in the semimoonlike features run parallel to the sides of the Gibbs triangle. The region indicated by the dark gray background and corresponds to a concave region in the free energy that is unstable against one type of concentration fluctuation (one $\lambda < 0$), so that phase separation will occur. This case corresponds with the following equation (cf. eq 10)

$$\begin{aligned}&(C - B)(-16C^2c_1c_2c_3 + 4(C + B)(c_1c_2 + c_2c_3 + c_1c_3)) \\ &\quad - 2B(c_1 + c_2 + c_3) - 1 \\ &> 0\end{aligned} \tag{61}$$

The curve separating the black and dark gray regions corresponds to the spinodal. It is also of importance to note that the critical curve starts to intersect with the Gibbs triangle in this concentration range, as shown by the open green circles (above the Gibbs triangle) changing in solid green circles (below the Gibbs triangle). The significance of the critical curve will be discussed later in this section. An interesting situation occurs at

$$c_{tot} = \frac{3B + 5C}{4C^2 - 2B(B + C)} \tag{62}$$

(see Figure 2b for c_{tot}=1.3 mol/m^3), which shows straight spinodals at mole fractions

$$x_i = \frac{B + C}{3B + 5C} \tag{63}$$

for which the sum of the other two mole fractions $x_j + x_k = 1 - x_i$ is constant (x_i= 3/13 in Figure 2b). This can be verified by substituting eq 63 in expression 10 for a_0. For a more detailed discussion, see Appendix A.4.

For $\frac{3B+5C}{4C^2-2B(B+C)} < c_{tot} < \frac{3}{2(C-B)}$, the stable/metastable black regions become isolated features, and the unstable dark gray regions become interconnected (see Figure 2c,d for c_{tot}=1.35 and 1.3728... mol/m^3 and diagrams for a number of additional concentrations in the Supporting Information, Figures S11−S15).

Three-Phase Region. A special case is shown in Figure 2d (at c_{tot}= 1.3728... mol/m^3) where adjacent binodals meet in three points leading to three local minima in the free energy surface (see Appendix A.4). These three local minima can be connected to form a triangle (yellow triangle in Figure 2d−f) in which any mixture will separate in three phases with a composition corresponding to the vertices of this triangle. The black region inside this triangle is metastable against phase separation, while the dark gray region represents an unstable region. Both regions will eventually phase separate, and therefore, the details of the local stability analysis are superfluous. However, the kinetics of phase separation may

https://doi.org/10.1021/acsomega.3c02604
ACS Omega 2023, 8, 28387−28408

reflect some aspects of the local stability landscape (Zhou et al.[16]).

The black region disappears when $c_{tot} = c_{1,c} + c_{2,c} + c_{3,c} = \frac{3}{2(C-B)}$ (see Figure 2e with c_{tot}=1.5 mol/m^3), where the tops of the three binodals coincide in one point. Previously, it was demonstrated that critical points of the form of eq 21 always satisfy the requirements that Det($\boldsymbol{M}_1$) = 0 and Det($\boldsymbol{M}_2$) = 0, provided that eq 23 applies (Appendix A.2). For the symmetric mixture, the requirement in eq 23 for the critical curve can be shown to result in the relation $S_{c,21} + S_{c,31} = 1$ (see Appendix A.4), which has multiple solutions and therefore does not represent a single tie-line but a plane in the (c_1, c_2, c_3)-space. Since the normal vector to this plane is unique, it is more convenient to characterize the plane by the normal vector.

Next, the critical curve is discussed, which is represented as open or filled green circles in Figure 2. For both regions, $\frac{1}{C-B} < c_{tot} < \frac{3B+5C}{4C^2-2B(B+C)}$ and $\frac{3B+5C}{4C^2-2B(B+C)} < c_{tot} < \frac{3}{2(C-B)}$, eq 23 can be written as

$$\begin{aligned}&(B - CS_{c,21} - CS_{c,31})^2 - S_{c,21}(C - BS_{c,21} - CS_{c,31})^2 \\ &\quad - S_{c,31}(C - CS_{c,21} - BS_{c,31})^2 \\ &= -B^2(S_{c,21}{}^3 + S_{c,31}{}^3) - (C^2 + 2BC) \\ &\quad (S_{c,21}{}^2 S_{c,31} + S_{c,21}S_{c,31}{}^2) + (C^2 + 2BC) \\ &\quad (S_{c,21}{}^2 + S_{c,31}{}^2) + (2C^2 + 2BC)S_{c,21}S_{c,31} \\ &\quad - (C^2 + 2BC)(S_{c,21} + S_{c,31}) + B^2 \\ &= 0 \end{aligned} \tag{64}$$

In Figure 3 solutions to eq 23 are plotted, where the black solid lines represent valid combinations for the critical tangents $S_{c,21}$ and $S_{c,31}$. The intersection of the solid black line with the gray dash-dotted lines features the solutions for the binary polymer mixture (black solid circles). The black dotted lines and gray dash-dotted lines demarcate boundaries where $c_{1,c}$, $c_{2,c}$, and $c_{3,c}$ switch signs (according to eqs 24−26) and $S_{c,21}$ = 0 and/or $S_{c,31}$ = 0, respectively). Physical solutions indicated by black dotted regions occur when $c_{1,c}$, $c_{2,c}$, $c_{3,c}$ all are positive, which is determined by the position of black dotted lines. Note that only a part of the ($S_{c,21}$,$S_{c,31}$) range is shown. These ($S_{c,21}$,$S_{c,31}$) combinations give rise to points on the critical curve shown in Figure 2 as green circles (open symbols: above the c_{tot} plane; filled symbols: below the c_{tot} plane). Points on the critical curve with a negative $S_{c,ij}$ indicate associative phase separation.

This critical curve also explains the dark gray regions of instability outside the semimoonlike in-Gibbs-triangle binodals in Figure 2b. The points on this critical curve are associated with out-of-Gibbs-triangle spinodals (and binodals) (see Appendix A.5). An example is shown in Figure 4, which can be found in the (c_1, c_3)-plane, and similar solutions can be found in the (c_1, c_2) and (c_2, c_3)-planes. Numerically, the solutions are found to converge slower than the in-Gibbs-triangle solutions because the free energy surface is almost completely flat in this region. Note that the binodal and spinodal are located slightly below the solid gray line at concentrations just below the critical point because the slopes of the tie-lines are not parallel to the Gibbs triangles. Consequently, the spinodal and binodal may appear at lower c_{tot} than the critical point itself.

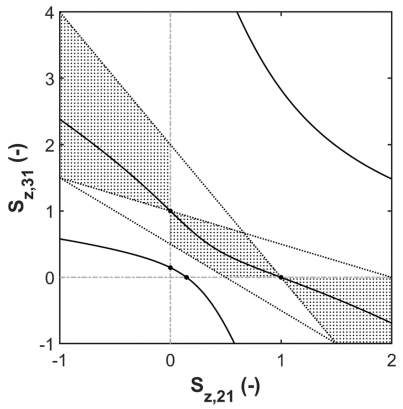

Figure 3. Regions indicating the physical relevant concentrations for the spinodal and critical coordinates in terms of the tangents $S_{z,21}$ and $S_{z,31}$ (with z = *sp*, *c* or *m*) and the relations between the critical tangents $S_{c,21}$ and $S_{c,31}$. (—): relation between $S_{c,21}$ and $S_{c,31}$ according to eq 22/23; (dotted region): physically relevant solutions, i.e., positive coordinates for the critical point or the spinodal surface (or the coordinates in eqs 46−48). The white regions indicate the parameter space where not all three critical point coordinates are positive, and where solutions are unphysical; (....): bounds to the physically relevant regions representing $c_{1,c} \geq 0$ (eq 24), $c_{2,c} \geq 0$ (eq 25), and $c_{3,c} \geq 0$ (eq 26); (●) the (physical *and* unphysical) solutions for binary mixtures (for $S_{c,21}$ = 0.146,1,6.85 or $S_{c,31}$ = 0.146,1,6.85), which can be found on the gray dash-dotted line that represent either $S_{c,31}$ = 0 or $S_{c,21}$ = 0. The plot was generated for maximally symmetric ternary mixture with pure virial coefficients $B = B_{ii}$ = 1 (m^3/mol), and cross virial coefficients $C = B_{ij}$ = 2 (m^3/mol).

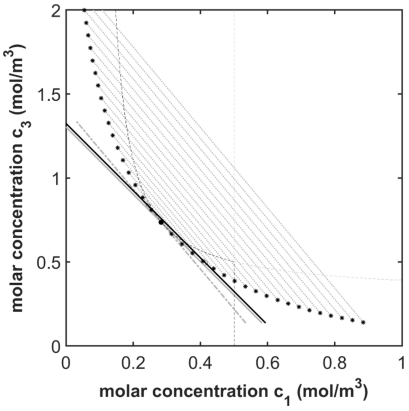

Figure 4. Out-of-plane binodal in the (c_1, c_3)-plane (or c_1 = c_2 plane) for the symmetric ternary mixture with pure virial coefficients $B = B_{ii}$ = 1 m^3/mol, and cross virial coefficients $C = B_{ij}$ = 2 m^3/mol: (gray ... lines) tie-lines; (*) end points of tie-lines at the binodal; (○) intersection of the binodal with the Gibbs triangle for c_{tot}=1.325 mol/m^3; (black and gray - - - line) spinodal, except for the vertical part of this curve; (gray -.-.- line) tangent to the spinodal and binodal in the critical point; (●) critical point; (gray — line) intersection with a Gibbs triangle through the critical point at c_{tot}=1.3 mol/m^3; The slopes of the tie-lines are not parallel to the Gibbs triangles. Therefore, the binodal and spinodal may appear at lower c_{tot} than represented by the solid gray line.

Increasing the concentration $c_{tot} > \frac{3}{2(C-B)}$ leads to the appearance of a white region (see Figure 2f with c_{tot}=1.6 mol/m^3 and Supporting Information, Figures S17−S22), which corresponds to the case where two λ < 0 is given by the inequalities (cf. eqs 11 and 12)

https://doi.org/10.1021/acsomega.3c02604
ACS Omega 2023, 8, 28387−28408

$$(C - B)(-16C^2c_1c_2c_3 + 4(C + B)(c_1c_2 + c_2c_3 + c_1c_3)) - 2B(c_1 + c_2 + c_3) - 1 < 0 \quad (65)$$

and

$$-12(C^2 - B^2)c_1c_2c_3 + 4B(c_1c_2 + c_2c_3 + c_1c_3) + (c_1 + c_2 + c_3) < 0 \quad (66)$$

corresponds to the white region that is unstable against two types of concentration fluctuations.

A stability analysis for a comparable model was published by Heidemann,[34] resulting in qualitatively similar figures (but without tie-lines): the above Figure 2a and the diagram for c_{tot} = 1.25 mol/m^3 (see Supporting Information, Figure S9) are comparable to Figures 1 and 2 by Heidemann (using $c_{tot} = \sqrt{\alpha/C}$).[34] With C = 2 m^3/mol and α= 2.5 and 3.5 mol/m^3, this leads to c_{tot}= 1.1 (Heidemann's Figure 1) and 1.32 mol/m^3 (Heidemann's Figure 2), respectively. These conditions compare to Figure 2a and a situation in-between Figure 2b and c in the present paper. Note that Figure 2c illustrates the topic of the discussion by Beegle et al.[35] and Heidemann[34] that in general the local curvature of the free energy surface is insufficient to predict global stability of the system. This is echoing statements made during the development of the theory of phase separation in the early 1900s.[30]

Huang et al.[15] also presented a phase diagram for a ternary mixture based on the Flory−Huggins−de Gennes mean-field theory. By comparing this model to the Edmond−Ogston model and equating the parameters for the critical point, the following relation is found

$$c_{tot} = \frac{N\chi}{2(C - B)} \quad (67)$$

linking the parameters for both models. Substituting eq 67 in their eq II.1b leads to a result identical to eq 1 for B = 0 and C = 1 (m^3/mol), leading to $c_{tot} = N\chi/2$ (Appendix A.1). It was found that the "large" triangle for the three-phase equilibrium appeared for both models at c_{tot} = 1.3728...(see Appendix A.4 in the present paper and Huang's Figure 1e that can be compared to the diagram at c_{tot} = 1.25 mol/m^3) (see Supporting Information, Figure S9).

This is in accordance with the calculation that the minimum of free energy coincides with the location where the binodals meet in the symmetric system (see Appendix A.4). The spinodals are straight lines for the present model for c_{tot} = 13/10 (Figure 2b) and for $N\chi/2$ = 4/3 in their model (Huang's Figure 1c), which is not the same but close. The existence of the proposed three-phase equilibria for the "small" triangles (see Huang's Figure b−d) was not supported by our work, as no local minima in the free energy surface were found. Unfortunately, neither Heidemann[34] nor Huang et al.[15] discussed the technical details of their calculations.

In the symmetric case, the coordinates $c_{i,s}$ in eqs 44−46 coincide with the critical point coordinates

$$c_{i,c} = \frac{1}{2(C - B)} \quad (68)$$

as was previously shown for binary mixtures.[8,10] This leads to solutions for the three phase systems that are very similar compared to those for the binary mixtures

$$\frac{c_i^K}{c_{i,c}} = -W_z\left(-\frac{c_i^K}{c_{i,c}} \cdot e^{-c_i^K/c_{i,c}}\right) \quad (69)$$

with K = I, II, or III and i = 1, 2, or 3 and z = −1 or 0. Equation 67 is solved in terms of the so-called Lambert-W function.[32] By convention, the phase rich in component 1 will be called phase I, the one rich in component 2 will be called phase II, and the one rich in component 3 will be called phase III. The phase rich in component i is represented by the z = −1 branch, and the phases depleted in component i are represented by the z = 0 branch of the Lambert-W function.

DISCUSSION

The current work can be extended in various directions. First, one could consider ternary mixtures where the virial coefficients for the pure components are identical, but the cross-virial coefficients differ. It is expected that in such systems, many of the features observed in the (maximally) symmetric ternary mixture are maintained qualitatively (e.g., semimoonlike regions, out-of-Gibbs-triangle binodals). Second, one could consider asymmetric mixtures, where all six virial coefficients differ. For such systems, the unstable and metastable regions can still be represented in terms of Gibbs triangles using eqs 10−12. The representation of the tie-lines, however, cannot simply be given by a set of stacked Gibbs triangles each characterized by a specific constant c_{tot} because the tie-lines will be out-of-Gibbs-triangle. For c_1, c_2, and c_3 large enough (formally c_1, c_2, $c_3 \to \infty$), the three coexisting phases will be all located in a plane defined by eq 55. Third, one could consider including third-order virial coefficients in the expressions for the Helmholtz free energy (eq 1), something that could be essential for some cases.[36] Fourth, the current work may be extended to cover examples of associative phase behavior for cases where one of the cross-virial coefficients is negative (and the related tangent is positive). Lastly, some of the results might be generalized to mixtures of N components (expression for the critical point, relation between the tangents to the critical curve, stability criteria using the Descartes rule of signs, and relation between the concentration of individual components in the different phases satisfying the Lambert-W function). That would make the present work useful as a stepping stone toward describing polydisperse and multicomponent mixtures. This would be relevant for describing phase separation phenomena in complex systems.

CONCLUSIONS

In this paper, an extension of the Edmond−Ogston theory describing phase separation in ternary polymer mixtures in a common solvent was considered. De facto, this makes these systems quaternary mixtures. Stacked Gibbs triangles can be used to represent the phase diagrams for the symmetric mixture, where the total polymer concentration serves as a parameter labeling the different Gibbs triangles. Ternary mixtures can also be considered as ideal examples for the case of three binary mixtures with shared components, as addressed in earlier work.[13]

Various novel analytical expressions were derived for the Edmond−Ogston model for ternary mixtures. A necessary condition for the virial coefficients for the occurrence of phase

https://doi.org/10.1021/acsomega.3c02604
ACS Omega 2023, 8, 28387−28408

separation in two or three phases was identified. An analytical expression was obtained to describe the relation between the tangents of the plane to the binodal and spinodal surface for each point on the critical curve. The Descartes sign rule was successfully applied to identify different regions of (local) thermodynamic instability. Similarly, as for binary mixtures, the Lambert-W functions were also found to play a central role in the description of the concentrations of the components in the coexisting phases of ternary mixtures. In addition, the tie-lines that connect the compositions of the coexisting phases are explicitly shown in our diagrams.

For maximally symmetric mixtures with $C > B > 0$, three regions in terms of phase behavior can be identified as a function of increasing total concentration. Typically, at low total concentrations, the three components are completely mixed. At intermediate total concentrations, two-phase systems will develop that are each equally enriched in the third component. At the highest concentrations, three-phase systems will develop that are each enriched in one of the components. For the maximally symmetric case, we have a mixed system for $c_{tot} < \frac{1}{C-B}$, two-phase systems for $\frac{1}{C-B} < c_{tot} < \frac{1.3728\ldots}{C-B}$, and three-phase systems for $c_{tot} > \frac{1.3728\ldots}{C-B}$. This means that the two-phase region for maximal symmetric mixtures occurs only over a narrow concentration range of the range of $\frac{0.3728\ldots}{C-B}$, which seems smaller than one might intuitively have expected. Qualitatively, this observation is expected to hold for other mixtures too (including asymmetric mixtures), though quantitatively, there will still be differences.

The expressions were numerically evaluated for symmetric mixtures, where the virial coefficients of the three pure components as well as the cross-virial coefficients are identical. The advantage of symmetric mixtures is that most, but not all, of the phase separation takes place in the plane of constant polymer concentration (referred to as "in-Gibbs-triangle"), thereby facilitating visualization. Analytical expressions were obtained for the binodals in these planes.

Surprisingly, not all phase separation phenomena take place in-Gibbs-triangle for maximally symmetric mixtures, as some of the tie-lines intersect the planes of constant concentration. This out-of-Gibbs-triangle behavior is found in a distinct region between the in-Gibbs-triangle binodals. The in-Gibbs-triangle binodals represent segregative phase separation, whereas the out-of-Gibbs-triangle binodals represent solutions where two components show associative and the third segregative phase separation. It appears that this partial associative phase separation has not been reported earlier.

A. APPENDICES

A.1. Comparison of Edmond–Ogston and Flory–Huggins–de Gennes for a Ternary Mixture in the Context of the Calculations by Huang et al.

The Edmond–Ogston model starts from the following expression for the Helmholtz free energy

$$\frac{F}{RTV} = c_1\ln(c_1) + c_2\ln(c_2) + c_3\ln(c_3) + B_{11}c_1^2 + B_{22}c_2^2 + B_{33}c_3^2 + 2B_{12}c_1c_2 + 2B_{13}c_1c_3 + 2B_{23}c_2c_3 \quad (70)$$

where the Flory–Huggins–de Gennes free energy model[15] reads

$$\frac{NF}{RTV} = \frac{\varphi_1\ln(\varphi_1)}{N_1/N} + \frac{\varphi_2\ln(\varphi_2)}{N_2/N} + \frac{\varphi_3\ln(\varphi_3)}{N_3/N} + N\chi_{12}\varphi_1\varphi_2 + N\chi_{13}\varphi_1\varphi_3 + N\chi_{23}\varphi_2\varphi_3 \quad (71)$$

where terms involving concentration gradients are ignored. N_i is the degree of polymerization of component i (and $N = N_1 = N_2 = N_3$ in the calculations of Huang et al.[15]), φ_i is the (local) composition of component i, and χ_{ij} is the interaction parameter between components i and j. Table 2 shows the matching of terms for the Edmond–Ogston and Flory–Huggins–de Gennes models.

Table 2. Matching of Terms for the Edmond–Ogston and Flory–Huggins–de Gennes Models

Edmond–Ogston	Flory–Huggins–de Gennes
c_1	φ_1
$B = B_{11} = B_{22} = B_{33}$	0
$2C = 2B_{12} = 2B_{13} = 2B_{23}$	$N\chi = N\chi_{12} = N\chi_{13} = N\chi_{23}$

To compare the calculations of Huang et al.[15] (Huang's Figure 1) directly to the present results (Figure 2), it is noted that there are two parameters here (C and c_{tot}), and only one in the work of Huang et al. ($N\chi$).

For most cases, the identification $c_{tot} = N\chi/2$ seems to give a fair match with the phase diagrams, although there is no formal justification for this. The minimal concentration c_{tot} = 1.3728... mol/m^3 to get three phases (yellow triangle) is the same between both models (Figure 2d in the present paper vs Huang's Figure 1e). Huang's Figure 1f and Figure 2e in the present paper are presented at the same concentration c_{tot} = 1.5 mol/m^3, where Figure 2e provides more details on the local stability.

For the straight spinodals (Huang's Figure 1c), the relation $c_{tot} = N\chi/2$ does not seems to hold. In Huang's calculation, straight spinodals (Huang's Figure 1c) are found for $N\chi = 8/3$, corresponding to $B = 0$ m^3/mol and $C = 4/3$ m^3/mol. According to eq 62, straight spinodals occur for c_{tot}= 15/16 mol/m^3 instead of 4/3 mol/m^3.

A.2. Determinants for M_1 and M_2 along the Critical Curve

Determinant $\boldsymbol{M}_1$ (eq 7) along the critical curve (eq 21) can be evaluated as

$$\det \boldsymbol{M}_1 = \det\begin{pmatrix} 2\sum_{i=2,3} B_{1i}S_{c,i1} & 2B_{12} & 2B_{13} \\ 2B_{12} & 2\sum_{i=1,3} B_{2i}S_{c,i2} & 2B_{23} \\ 2B_{13} & 2B_{23} & 2\sum_{i=1,2} B_{3i}S_{c,i3} \end{pmatrix}$$
$$= 8\{B_{12}^2B_{13}S_{c,13} + B_{12}^2B_{23}S_{c,23} - B_{12}B_{13}B_{23} + B_{23}^2B_{12}S_{c,21} + B_{13}^2B_{12}S_{c,12} - B_{12}B_{13}B_{23} + B_{13}^2B_{23}S_{c,32} + B_{23}^2B_{13}S_{c,31} - B_{12}^2B_{13}S_{c,13} - B_{12}^2B_{23}S_{c,23} + B_{12}B_{13}B_{23} - B_{23}^2B_{12}S_{c,21} - B_{13}^2B_{12}S_{c,12} + B_{12}B_{13}B_{23} - B_{13}^2B_{23}S_{c,32} - B_{23}^2B_{13}S_{c,31}\} = 0 \quad (72)$$

confirming that Det $\boldsymbol{M}_1 = 0$ for every point along the critical curve. For Det $\boldsymbol{M}_2''' = 0$ along the critical curve, one has

https://doi.org/10.1021/acsomega.3c02604
ACS Omega 2023, 8, 28387−28408

$$\mathrm{Det}\,\boldsymbol{M}_2''' = \mathrm{Det}\begin{pmatrix} 2B_{12}S_{c,21} + 2B_{13}S_{c,31} & 2B_{12} & 2B_{13} \\ 2B_{12} & 2B_{12}S_{c,12} + 2B_{23}S_{c,32} & 2B_{23} \\ \frac{4}{c_{1,c}^{\,2}}\left\{{B_{23}}^2 - \left(\sum_{i=1,3} B_{2i}S_{c,i2}\right)\left(\sum_{i=1,2} B_{3i}S_{c,i3}\right)\right\} & \frac{4}{c_{2,c}^{\,2}}\left\{{B_{13}}^2 - \left(\sum_{i=2,3} B_{1i}S_{c,i1}\right)\left(\sum_{i=1,2} B_{3i}S_{c,i3}\right)\right\} & \frac{4}{c_{3,c}^{\,2}}\left\{{B_{12}}^2 - \left(\sum_{i=2,3} B_{1i}S_{c,i1}\right)\left(\sum_{i=1,3} B_{2i}S_{c,i2}\right)\right\} \end{pmatrix}$$

where the expression for $\mathrm{Det}\boldsymbol{M}_2'''$ is given in eq 20, and for $\mathrm{Det}\boldsymbol{M}_2'$ and $\mathrm{Det}\boldsymbol{M}_2''$ as

$$\begin{aligned} c_1^2c_2^2c_3^2\mathrm{Det}\boldsymbol{M}_2' = {} & (4B_{23}B_{12}c_2c_1 - 2B_{13}c_1(1 + 2B_{22}c_2)\,) \\ & (4{B_{12}}^2c_2c_1 - (1 + 2B_{22}c_2)(1 + 2B_{11}c_1)) \\ & -\,(\,4{B_{23}}^2c_2c_3 - (1 + 2B_{22}c_2) \\ & (1 + 2B_{33}c_3))(4{B_{23}}^2c_2c_3 - (1 + 2B_{22}c_2) \\ & (1 + 2B_{33}c_3)) + (4B_{23}B_{13}c_3c_1 \\ & - 2B_{12}c_1(1 + 2B_{33}c_3)\,) \\ & (4{B_{13}}^2c_3c_1 - (1 + 2B_{33}c_3)(1 + 2B_{11}c_1)) \end{aligned} \tag{73}$$

$$\begin{aligned} c_1^2c_2^2c_3^2\mathrm{Det}\boldsymbol{M}_2'' = {} & (4B_{13}B_{23}c_3c_2 - 2B_{12}c_2(1 + 2B_{33}c_3)\,) \\ & (4{B_{23}}^2c_3c_2 - (1 + 2B_{33}c_3)(1 + 2B_{22}c_2)) \\ & -\,(4{B_{13}}^2c_3c_1 - (1 + 2B_{33}c_3)(1 + 2B_{11}c_1)) \\ & (4{B_{13}}^2c_3c_1 - (1 + 2B_{33}c_3)(1 + 2B_{11}c_1)) \\ & +\,(4B_{13}B_{12}c_1c_2 - 2B_{23}c_2(1 + 2B_{11}c_1)) \\ & (4{B_{12}}^2c_1c_2 - (1 + 2B_{11}c_1)(1 + 2B_{22}c_2)) \end{aligned} \tag{74}$$

Consciously not substituting the explicit expressions for all critical coordinates on the bottom row, the above equation can be written in the same way as

$$\begin{aligned} & \frac{S_{c,11}^3}{c_{1,c}^{\,2}} + \frac{S_{c,21}^3}{c_{2,c}^{\,2}} + \frac{S_{c,31}^3}{c_{3,c}^{\,2}} \\ & = -\frac{{S_{c,21}}^2{S_{c,31}}^2}{16\{B_{12}B_{13} - B_{12}B_{23}S_{c,21} - B_{13}B_{23}S_{c,31}\}^2}\mathrm{Det}\boldsymbol{M}_2' \\ & = -\frac{S_{c,21}{S_{c,31}}^2}{16\{B_{12}B_{13} - B_{12}B_{23}S_{c,21} - B_{13}B_{23}S_{c,31}\}^2}\mathrm{Det}\boldsymbol{M}_2'' \\ & = -\frac{{S_{c,21}}^2S_{c,31}}{16\{B_{12}B_{13} - B_{12}B_{23}S_{c,21} - B_{13}B_{23}S_{c,31}\}^2}\mathrm{Det}\boldsymbol{M}_2''' = 0 \end{aligned} \tag{75}$$

Note that $S_{c,11} \equiv -1$. The expressions in terms of $\mathrm{Det}\boldsymbol{M}_2'$ and $\mathrm{Det}\boldsymbol{M}_2''$ are given in eq 75 to demonstrate that eqs 20, 73, and 74 eventually lead to the same relation.

A.3. Criterion for the Virial Coefficients for the Occurrence of Two Negative Eigenvalues Anywhere in the Phase Diagram

Introducing

$$b_{12} = \sqrt{\frac{{B_{12}}^2}{B_{11}B_{22}}};\; b_{13} = \sqrt{\frac{{B_{13}}^2}{B_{11}B_{33}}};\; b_{23} = \sqrt{\frac{{B_{23}}^2}{B_{22}B_{33}}} \tag{76}$$

Equations 29 and 31 can be written as

$${b_{12}}^2 + {b_{13}}^2 + {b_{23}}^2 < 2b_{12}b_{13}b_{23} + 1 \tag{77}$$

and

$$\begin{aligned} & B_{11}B_{22}\{{b_{12}}^2 - 1\} + B_{11}B_{33}\{{b_{13}}^2 - 1\} + B_{22}B_{33}\{{b_{23}}^2 - 1\} \\ & > 0 \end{aligned} \tag{78}$$

Equation 77 can be rewritten as

$${b_{23}}^2 - 2b_{12}b_{13}b_{23} + {b_{12}}^2{b_{13}}^2 < {b_{12}}^2{b_{13}}^2 - {b_{12}}^2 - {b_{13}}^2 + 1 \tag{79}$$

leading to

$$(b_{23} - b_{12}b_{13})^2 < ({b_{12}}^2 - 1)({b_{13}}^2 - 1) \tag{80}$$

and also

$$\begin{aligned} & b_{12}b_{13} - \sqrt{({b_{12}}^2 - 1)({b_{13}}^2 - 1)} \\ & < b_{23} \\ & < b_{12}b_{13} + \sqrt{({b_{12}}^2 - 1)({b_{13}}^2 - 1)} \end{aligned} \tag{81}$$

Two cases can be identified: case 1 where $(b_{12} > 1) \wedge (b_{13} > 1) \wedge (b_{23} > 1)$ and case 2 where $(0 < b_{12} < 1) \wedge (0 < b_{13} < 1) \wedge (0 < b_{23} < 1)$. Note that we exclude the cases where $(b_{12} > 1) \wedge (0 < b_{13} < 1)$ or $(0 < b_{12} < 1) \wedge (b_{13} > 1)$, which give rise to imaginary solutions to b_{23}. Furthermore, the cases where $(b_{12} < 0)$ and/or $(b_{13} < 0)$ are excluded because all virial coefficients are assumed to be positive. Also note that $b_{12} = b_{13} = b_{23} = 1$ is not a solution because of the inequality in eq 77.

In case 1, if $(b_{12} > 1) \wedge (b_{13} > 1)$, it follows that $(b_{23} > 1)$. For this, the following needs to be proven for the lower limit of eq 81:

$$b_{23} > b_{12}b_{13} - \sqrt{({b_{12}}^2 - 1)({b_{13}}^2 - 1)} \geq 1 \tag{82}$$

The right-hand side of this equation can be simplified to

$$b_{12}b_{13} - 1 \geq \sqrt{({b_{12}}^2 - 1)({b_{13}}^2 - 1)} \tag{83}$$

or

$$(b_{12}b_{13} - 1)^2 \geq ({b_{12}}^2 - 1)({b_{13}}^2 - 1) \tag{84}$$

eventually leading to the true statement

$$(b_{12} - b_{13})^2 \geq 0 \tag{85}$$

proving the right-hand side of eq 82. By extension, this also proves that $b_{23} > 1$ in the left-hand side of eq 82.

In case 2, if $(0 < b_{12} < 1) \wedge (0 < b_{13} < 1)$, it follows that $(0 < b_{23} < 1)$. For this, the following needs to be proven for the upper limit of eq 81:

$$b_{23} < b_{12}b_{13} + \sqrt{({b_{12}}^2 - 1)({b_{13}}^2 - 1)} \leq 1 \tag{86}$$

The right-hand side of this equation can be simplified to

$$b_{12}b_{13} - 1 \leq -\sqrt{({b_{12}}^2 - 1)({b_{13}}^2 - 1)} \tag{87}$$

https://doi.org/10.1021/acsomega.3c02604
ACS Omega 2023, 8, 28387−28408

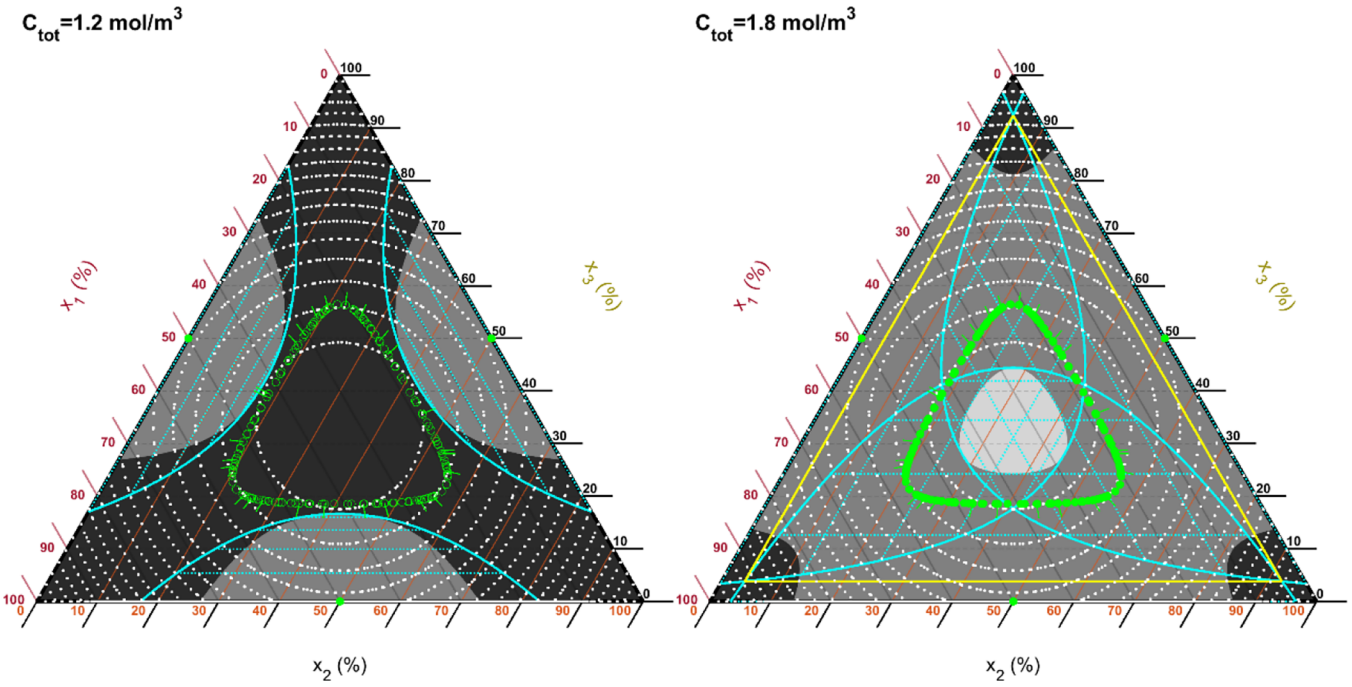

Figure 5. White dotted lines: Examples of the iso-osmotic pressure contours in phase diagrams for c_{tot} = 1.2 and 1.8 mol/m^3 and B = 1 m^3/mol, C = 2 m^3/mol. Open green circles: critical points above the plane of constant c_{tot}. Solid green circles: critical points below the plane of constant c_{tot}. Short green solid lines: projection of the tangent to the critical plane to the Gibbs triangle according to Appendix A.5). Yellow lines: triangle with three phases in equilibrium; Cyan solid lines: binodals; Cyan dotted lines: tie-lines; Light gray: two negative eigenvalues; Dark gray: one negative eigenvalue; Black region: zero negative eigenvalues.

or

$$(b_{12}b_{13} - 1)^2 \geq ({b_{12}}^2 - 1)({b_{13}}^2 - 1) \tag{88}$$

The sign of the inequality changes because both terms in eq 87 are negative for $(0 < b_{12} < 1) \wedge (0 < b_{13} < 1)$, eventually leading to the true statement

$$(b_{12} - b_{13})^2 \geq 0 \tag{89}$$

proving the right-hand side of eq 86. By extension, this also proves that $b_{23} < 1$ in the left-hand side of eq 86.

It is noted that although eq 77 is satisfied in cases 1 and 2, the inequality in eq 78 is never satisfied in case 2. Therefore, two negative eigenvalues can only occur in case 1, when $(b_{12} > 1) \wedge (b_{13} > 1) \wedge (b_{23} > 1)$.

Alternatively, if we have the requirement that $a_0 > 0$, it implies that not all three criteria $(b_{12} > 1)$, $(b_{13} > 1)$, and $(b_{23} > 1)$ can be satisfied simultaneously.

A.4. Expressions for the In-Gibbs-Triangle Binodals (Maximally Symmetric Mixture)

(a) Expressions for the in-Gibbs-triangle binodals for N = 3 and P = 2

The full expressions for the osmotic pressure Π and chemical potential μ_i of component i = 1, 2, or 3 for the maximally symmetric mixture can be written as

$$\frac{\Pi}{RT} = -\frac{1}{RT}\left(\frac{\partial F}{\partial V}\right)_{T,n_1,n_2,n_3} = (B - C)({c_1}^2 + {c_2}^2 + {c_3}^2) + (Cc_{tot} + 1)c_{tot} \tag{90}$$

$$\frac{\mu_i}{RT} = \frac{1}{RT}\left(\frac{\partial F}{\partial n_i}\right)_{T,V,n_j,n_k} = \ln c_i + 2(B - C)c_i + 2Cc_{tot} + 1 \tag{91}$$

where $c_{tot} = c_1 + c_2 + c_3$. The last two terms in the above equations are constant for fixed c_{tot} and can be ignored, when discussing the coexisting phases, where they cancel. Equation 90 indicates that all compositions with the same osmotic pressure can be found on a circle within the Gibbs triangle (see Figure 5). For constant c_{tot},

$$c_1^{I2} + c_2^{I^2} + c_3^{I^2} = c_1^{II^2} + c_2^{II^2} + c_3^{II^2} \tag{92}$$

Equation 91 indicates that phase compositions with the same chemical potential need to satisfy the equality

$$\ln c_i^{I} - 2(C - B)c_i^{I} = \ln c_i^{II} - 2(C - B)c_i^{II} \tag{93}$$

which gives rise to solutions in terms of Lambert-W functions. It follows from eq 93 that

$$W(-(c_i^{I}/c_{i,c})\, e^{-(c_i^{I}/c_{i,c})}) = W(-(c_i^{II}/c_{i,c})\, e^{-(c_i^{II}/c_{i,c})}) \tag{94}$$

with $c_{i,c} = \frac{1}{2(C-B)}$, where the appropriate branch of the Lambert-W should be chosen. Note here that the concentrations can be on the same branch of the Lambert-W function (i.e., the component is evenly distributed over both phases), or they can be on separate branches (i.e., the component has a high concentration in one phase and a low concentration in the other).

We can check now whether the equation that we derived using heuristic arguments fits the equation.

https://doi.org/10.1021/acsomega.3c02604
ACS Omega 2023, 8, 28387−28408

Consider the binodal emerging from the $c_3 = 0$ axis while considering that $c_{1,c} = c_{2,c} = c_{3,c}$ for the maximally symmetric case. The in-Gibbs-triangle binodal coordinates for the maximally symmetric ternary mixture are as follows:

For the left branch (for $c_{2,bi} \geq c_{2,c}$, phase I),

$$\left(-c_{2,c}W_0\left(-\frac{c_{2,bi}}{c_{2,c}}e^{-c_{2,bi}/c_{2,c}}\right), -c_{2,c}W_{-1}\left(-\frac{c_{2,bi}}{c_{2,c}}e^{-c_{2,bi}/c_{2,c}}\right), c_{tot} - \left(-c_{2,c}W_{-1}\left(-\frac{c_{2,bi}}{c_{2,c}}e^{-c_{2,bi}/c_{2,c}}\right) - c_{2,c}W_0\left(-\frac{c_{2,bi}}{c_{2,c}}e^{-c_{2,bi}/c_{2,c}}\right)\right)\right) \quad (95)$$

For the right branch (for $c_{2,bi} \leq c_{2,c}$, phase II),

$$\left(-c_{2,c}W_{-1}\left(-\frac{c_{2,bi}}{c_{2,c}}e^{-c_{2,bi}/c_{2,c}}\right), -c_{2,c}W_0\left(-\frac{c_{2,bi}}{c_{2,c}}e^{-c_{2,bi}/c_{2,c}}\right), c_{tot} - \left(-c_{2,c}W_{-1}\left(-\frac{c_{2,bi}}{c_{2,c}}e^{-c_{2,bi}/c_{2,c}}\right) - c_{2,c}W_0\left(-\frac{c_{2,bi}}{c_{2,c}}e^{-c_{2,bi}/c_{2,c}}\right)\right)\right) \quad (96)$$

Filling in these coordinates in eq 92 leads to

$$\begin{aligned}&\left(-c_{2,c}W_0\left(-\frac{c_{2,bi}}{c_{2,c}}e^{-c_{2,bi}/c_{2,c}}\right)\right)^2 + \left(-c_{2,c}W_{-1}\left(-\frac{c_{2,bi}}{c_{2,c}}e^{-c_{2,bi}/c_{2,c}}\right)\right)^2 + \left(c_{tot} - \left(-c_{2,c}W_{-1}\left(-\frac{c_{2,bi}}{c_{2,c}}e^{-c_{2,bi}/c_{2,c}}\right) - c_{2,c}W_0\left(-\frac{c_{2,bi}}{c_{2,c}}e^{-c_{2,bi}/c_{2,c}}\right)\right)\right)^2 \\ &= \left(-c_{2,c}W_{-1}\left(-\frac{c_{2,bi}}{c_{2,c}}e^{-c_{2,bi}/c_{2,c}}\right)\right)^2 + \left(-c_{2,c}W_0\left(-\frac{c_{2,bi}}{c_{2,c}}e^{-c_{2,bi}/c_{2,c}}\right)\right)^2 + \left(c_{tot} - \left(-c_{2,c}W_{-1}\left(-\frac{c_{2,bi}}{c_{2,c}}e^{-c_{2,bi}/c_{2,c}}\right) - c_{2,c}W_0\left(-\frac{c_{2,bi}}{c_{2,c}}e^{-c_{2,bi}/c_{2,c}}\right)\right)\right)^2\end{aligned} \quad (97)$$

which is true. Therefore, the expression for the binodal is exact for the binodal on the $c_{1,bi} + c_{2,bi} + c_{3,bi} = c_{tot}$ plane, originating from the $c_3 = 0$ axis.

Simplifying the notation of eqs 95 and 96 leads to

$$(c_1^{I}, c_2^{I}, c_3^{I}) = (x_1^{I}, x_2^{I}, 1 - x_1^{I} - x_2^{I})c_{tot} \quad (98)$$

$$(c_1^{II}, c_2^{II}, c_3^{II}) = (x_2^{I}, x_1^{I}, 1 - x_1^{I} - x_2^{I})c_{tot} \quad (99)$$

with x_i^K the mole fraction of component i in phase K (= I or II) and where $0 < x_2^{I} < \frac{1}{3}$ and where the other two pairs of coexisting phases can be found under cyclic permutation of the concentrations. As a result, eq 93 reduces into a single equation

$$(C - B)c_{tot} = \frac{1}{2(x_1^{I} - x_2^{I})}\ln\left(\frac{x_1^{I}}{x_2^{I}}\right) \quad (100)$$

from which the two coexisting phases can be determined as a function of c_{tot}. To follow the perpendicular bisector from the center of the Gibbs triangle toward the midpoint of one of its sides (i.e., $x_1^{I} = x_2^{I}$ and $x_3^{I} = 0$), one takes $x_1^{I} \to \frac{1}{2}$. Using L'Hôpital's rule, one finds

$$(C - B)c_{tot} = \lim_{x_1^{I} \to 1/2} \frac{-\frac{1}{(1 - x_1^{I})} - \frac{1}{x_1^{I}}}{-4} = 1 \quad (101)$$

leading to

$$\begin{aligned}(c_1^{I}, c_2^{I}, c_3^{I}) = (c_1^{II}, c_2^{II}, c_3^{II}) &= \left(\frac{1}{2}, \frac{1}{2}, 0\right)c_{tot} \\ &= \left(\frac{1}{2(C - B)}, \frac{1}{2(C - B)}, 0\right)\end{aligned} \quad (102)$$

These concentrations correspond to the critical point for binary symmetric mixtures (Dewi et al.[8,9]).

(b) Composition of coexisting phases for the binary mixtures at c_{tot}

The intersection of the binodal with the sides of the Gibbs triangle can be calculated as

$$c_{tot} - \left(-c_{2,c}W_{-1}\left(-\frac{c_{2,bi}}{c_{2,c}}e^{-c_{2,bi}/c_{2,c}}\right) - c_{2,c}W_0\left(-\frac{c_{2,bi}}{c_{2,c}}e^{-c_{2,bi}/c_{2,c}}\right)\right) = 0 \quad (103)$$

as follows directly from setting $c_{3,\,bi} = 0$ in eq 95 or 96.

(c) Straight spinodal lines in the phase diagram for the maximally symmetric mixture (cf. Figure 2b)

Starting from the expression for the spinodal, eqs 10 and 11 (but not expressed as an inequality) and assuming the conditions for the maximally symmetric model ($B = B_{11} = B_{22} = B_{33}$ and $C = B_{12} = B_{13} = B_{23}$) result in

$$\begin{aligned}a_0 \equiv\ &4C^2c_2c_3(1 + 2Bc_1) + 4C^2c_1c_3(1 + 2Bc_2) \\ &+ 4C^2c_1c_2(1 + 2Bc_3) - 16C^3c_1c_2c_3 \\ &- (1 + 2Bc_1)(1 + 2Bc_2)(1 + 2Bc_3) \\ =\ &0\end{aligned} \quad (104)$$

Converting the molar concentrations c_i to molar fractions x_i

$$c_i = x_i c_{tot} \quad (105)$$

https://doi.org/10.1021/acsomega.3c02604
ACS Omega 2023, 8, 28387−28408

and introducing the following simplifications and substitutions

$$x_1 + x_2 + x_3 = 1 \tag{106}$$

$$x_3 = a \text{ or } x_1 + x_2 + a = 1 \text{ or } x_2 = ((1 - a) - x_1) \tag{107}$$

lead to a polynomial in x_i

$$4(B - C)\left\{\left(\frac{1}{c_{tot}} + 2aB\right)(B + C) - 4aC^2\right\}{x_1}^2 - 4(1 - a)(B - C)\left\{\left(\frac{1}{c_{tot}} + 2aB\right)(B + C) - 4aC^2\right\}x_1 - 4\frac{a(1 - a)(B^2 - C^2)}{c_{tot}} - 2\frac{B}{{c_{tot}}^2} - \frac{1}{{c_{tot}}^3} = 0 \tag{108}$$

which should be true for all values of x_1; so, $a = 1$ and $c_{tot} = 0$ are not acceptable solutions, and $B = C$ does not satisfy the phase separation criterion. Therefore, the coefficients of the polynomial should be zero. So, for the coefficients of the first two terms of the polynomial,

$$\left(\frac{1}{c_{tot}} + 2aB\right)(B + C) - 4aC^2 = 0 \tag{109}$$

or

$$a = \frac{(B + C)}{4C^2 - 2B(B + C)}\frac{1}{c_{tot}} \tag{110}$$

Filling in a in the coefficient for the third term of the polynomial (which also should be zero) leads to

$$c_{tot} = \frac{3B + 5C}{4C^2 - 2B(B + C)} \tag{111}$$

and

$$a = \frac{B + C}{3B + 5C} \tag{112}$$

It is noted that it is not possible to write eq 111 only in terms of $(B - C)$, as is the case for the coexistence equation. Although all binodals are identical for $(C - B)$ = constant, the spinodal surfaces differ.

(d) Conditions for the formation of three phases (in-Gibbs-triangle binodals, $N = 3$ and $P = 3$)

For the in-Gibbs-triangle solutions for $N = 3$ and $P = 3$, we conjecture a solution for the concentrations in phases I, II, and III, inspired by the symmetry of the problem of the form

$$(c_1^{I}, c_2^{I}, c_3^{I}) = (x_2^{I}, x_2^{I}, 1 - 2x_2^{I})c_{tot} \tag{113}$$

$$(c_1^{II}, c_2^{II}, c_3^{II}) = (x_2^{I}, 1 - 2x_2^{I}, x_2^{I})c_{tot} \tag{114}$$

$$(c_1^{III}, c_2^{III}, c_3^{III}) = (1 - 2x_2^{I}, x_2^{I}, x_2^{I})c_{tot} \tag{115}$$

where $0 \le x_2^{I} \le \frac{1}{3}$. Using this form, the requirement for the osmotic pressure is automatically fulfilled. For the chemical potentials, one needs to fulfill eq 3, leading to a single expression

$$(C - B)c_{tot} = \frac{1}{(2 - 6x_2^{I})}\ln\left(\frac{1 - 2x_2^{I}}{x_2^{I}}\right) \tag{116}$$

In Figure 6, $(C - B)c_{tot}$ is plotted against x_2^{I}. At $x_2^{I} = 0.2076...$, there is a local minimum at $(C - B)c_{tot} =$

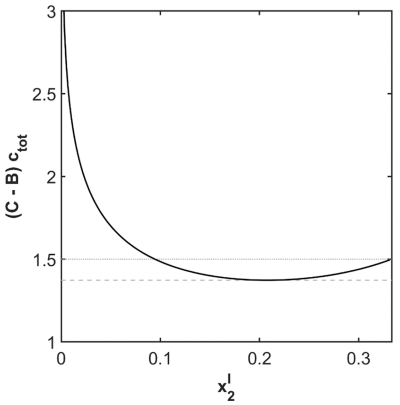

Figure 6. Plot of (—) $(C - B)c_{tot}$ as a function of x_2^{I}, showing a local minimum at $x_2^{I} = 0.2076$ where $(C - B)c_{tot} = 1.3728$ and at $x_2^{I} = \frac{1}{3}$, $(C - B)c_{tot} = \frac{3}{2}$. Furthermore, $(C - B)c_{tot} \to \infty$, when $x_2^{I} \downarrow 0$. For $1.3728 \le (C - B)\, c_{tot} \le \frac{3}{2}$ there are two possible x_2^{I} values that corresponding to a certain $(C - B)\, c_{tot}$, where the lowest x_2^{I}-value corresponds to the lowest free energy; (−--) horizontal line with $(C - B)c_{tot} = 1.3728$; (....) horizontal line with $(C - B)c_{tot} = 1.5$.

1.3728..., expressing a necessary condition for the formation of three phases. For $1.3728... \le (C - B)c_{tot} \le \frac{3}{2}$, there are two possible x_2^{I} values that correspond to a certain $(C - B)c_{tot}$. This is also reflected in Figure 2d, where the binodals intersect each other in two points for $c_{tot}(C - B) \ge 1.3728...$. Here, the smallest x_2^{I} of the possible x_2^{I} values should be chosen since this x_2^{I} value corresponds to the lowest Helmholtz free energy of the two. With each x_2^{I} value, three coexisting phases are associated, forming the corners of a triangle within the Gibbs triangle that defines the three-phase area. Using L'Hôpital's rule, one can establish the following limit for $x_2^{I} \to \frac{1}{3}$

$$(C - B)c_{tot} = \lim_{x_2^{I} \to 1/3} \frac{1}{(2 - 6x_2^{I})}\ln\left(\frac{1 - 2x_2^{I}}{x_2^{I}}\right) = \frac{\lim_{x_2^{I} \to 1/3}\left(\frac{-1}{(1 - 2x_2^{I})x_2^{I}}\right)}{\lim_{x_2^{I} \to 1/3}(-6)} = \frac{1}{6}\frac{1}{(1 - 2x_2^{I})x_2^{I}} = \frac{3}{2} \tag{117}$$

where all three phases collapse in a single point $(c_1, c_2, c_3) = \left(\frac{1}{3}, \frac{1}{3}, \frac{1}{3}\right)c_{tot}$

$$= \left(\frac{1}{2(C - B)}, \frac{1}{2(C - B)}, \frac{1}{2(C - B)}\right)$$

However, this point corresponds to a local maximum in the free energy.

The solutions above are the consequence of intersections of the in-Gibbs-triangle binodals. From the discussion above, it can be concluded that there are generally zero, one, or two solutions: zero if the binodals

https://doi.org/10.1021/acsomega.3c02604
ACS Omega 2023, 8, 28387−28408

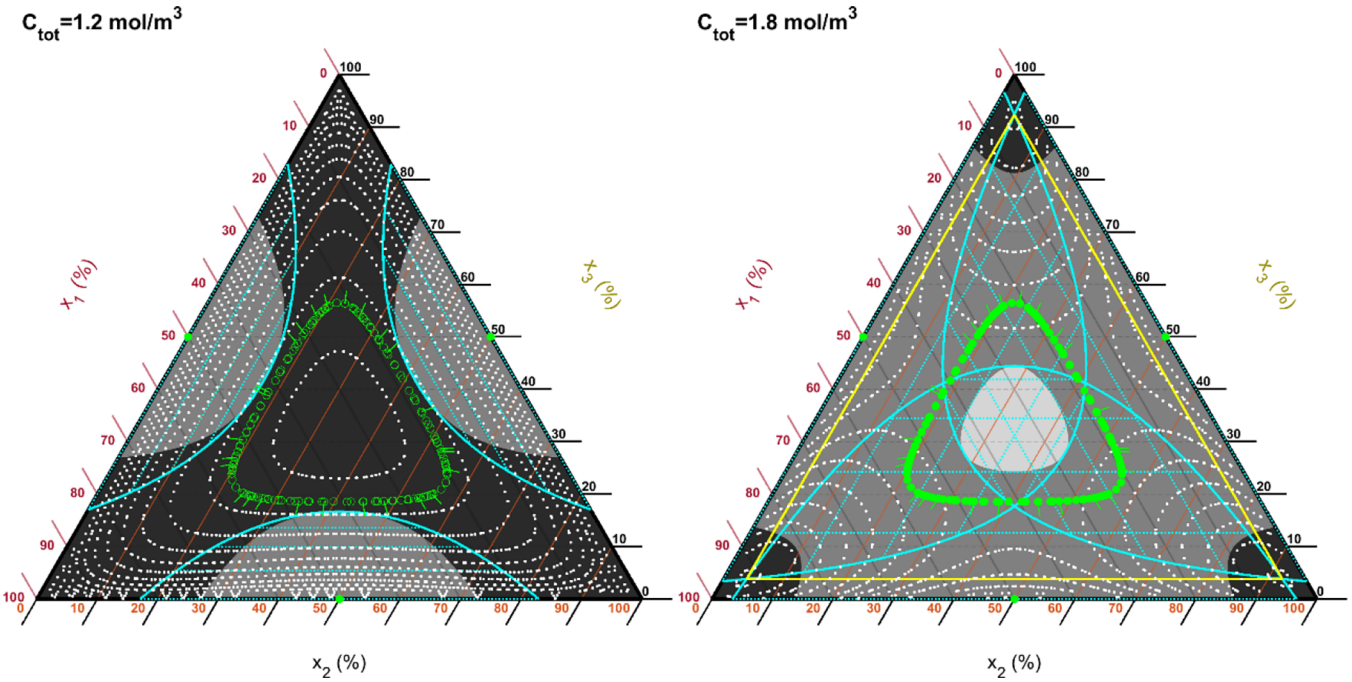

Figure 7. White dotted lines: Examples of the iso-free energy contours in phase diagrams for c_{tot} = 1.2 and 1.8 mol/m^3 and B = 1 m^3/mol, C = 2 m^3/mol. Open green circles: critical points above the plane of constant c_{tot}. Solid green circles: critical points below the plane of constant c_{tot}. Short green solid lines: projection of the tangent to the critical plane to the Gibbs triangle according to Appendix A.5). Yellow lines: triangle with three phases in equilibrium; Cyan solid lines: binodals; Cyan dotted lines: tie-lines; Light gray: two negative eigenvalues; Dark gray: one negative eigenvalue; Black region: zero negative eigenvalues.

do not intersect, one if they merely touch, and two if they fully intersect. In the case of two solutions, the largest solution for $c_{2,bi}$ of the pair is the one needed (the other describes the solution for the intersection closer to the center of the Gibbs triangle).

An example of the free energy surface is shown in Figure 7. The dashed white lines represent the contour lines of the free energy surface. At c_{tot} = 1.2 mol/m^3, the free energy varies relatively smoothly (featuring a concave area in the spinodal area), whereas at c_{tot}=1.8 mol/m^3, pronounced minima can be observed at the vertices of the Gibbs triangle.

A special case occurs when c_{tot} is chosen such that eq 125 has a single solution (cf. Figure 2d).

$$c_{tot} = c_{2,c}\left(-W_{-1}\left(-\frac{c_{2,bi}}{c_{2,c}}e^{-c_{2,bi}/c_{2,c}}\right) - 2W_0\left(-\frac{c_{2,bi}}{c_{2,c}}e^{-c_{2,bi}/c_{2,c}}\right)\right) \tag{118}$$

When two binodals intersect (previous section), a different pair of intersections will be found for each value of c_{tot}. Moving to lower c_{tot} will give a curve of intersections, with two branches merging in a point (and c_{tot}) where only a single intersection exists. This intersection is characterized by the criterion $\frac{dc_{tot}}{dc_{2,bi}} = \frac{1}{c_{tot}}\frac{dc_{tot}}{dx_2^1} = 0$ (see Figure 6). This point can be found by solving

$$\frac{dc_{tot}}{dc_{2,bi}} = c_{2,c}\left(-\frac{dW_{-1}\left(-\frac{c_{2,bi}}{c_{2,c}}e^{-c_{2,bi}/c_{2,c}}\right)}{d-\frac{c_{2,bi}}{c_{2,c}}e^{-c_{2,bi}/c_{2,c}}}\frac{d\left(-\frac{c_{2,bi}}{c_{2,c}}e^{-c_{2,bi}/c_{2,c}}\right)}{dc_{2,bi}} - 2\frac{dW_0\left(-\frac{c_{2,bi}}{c_{2,c}}e^{-c_{2,bi}/c_{2,c}}\right)}{d-\frac{c_{2,bi}}{c_{2,c}}e^{-c_{2,bi}/c_{2,c}}}\frac{d\left(-\frac{c_{2,bi}}{c_{2,c}}e^{-c_{2,bi}/c_{2,c}}\right)}{dc_{2,bi}}\right)$$
$$= \left(-\frac{W_{-1}\left(-\frac{c_{2,bi}}{c_{2,c}}e^{-c_{2,bi}/c_{2,c}}\right)}{\left(1+W_{-1}\left(-\frac{c_{2,bi}}{c_{2,c}}e^{-c_{2,bi}/c_{2,c}}\right)\right)} - 2\frac{W_0\left(-\frac{c_{2,bi}}{c_{2,c}}e^{-c_{2,bi}/c_{2,c}}\right)}{\left(1+W_0\left(-\frac{c_{2,bi}}{c_{2,c}}e^{-c_{2,bi}/c_{2,c}}\right)\right)}\right)\left(\frac{1}{c_{2,c}}e^{-c_{2,bi}/c_{2,c}}\right) = 0 \tag{119}$$

where the identity $dW_i(z)/dz = W_i(z)/(z(1 + W_i(z)))$ was used.

Another case occurs when c_{tot} is chosen such that eq 125 has two solutions (cf. Figure 2e and beyond). If the $(c_{3,\,bi} \le c_{3,\,c})$ branch of the binodal originating from the c_1 = 0 axis intersects the $(c_{2,\,bi} \ge c_{2,\,c})$ branch of the binodal originating from the c_3 = 0 axis (right bottom

https://doi.org/10.1021/acsomega.3c02604
ACS Omega 2023, 8, 28387−28408

corner of the Gibbs triangle), it is found that for $c_{2,\,bi} \geq c_{2,\,c}$

$$\left(c_{\mathrm{tot}} - \left(-c_{2,c}W_{-1}\left(-\frac{c_{2,bi}}{c_{2,c}}\mathrm{e}^{-c_{2,bi}/c_{2,c}}\right) - c_{3,c}W_0\left(-\frac{c_{2,bi}}{c_{2,c}}\mathrm{e}^{-c_{2,bi}/c_{2,c}}\right)\right), -c_{2,c}W_{-1}\left(-\frac{c_{2,bi}}{c_{2,c}}\mathrm{e}^{-c_{2,bi}/c_{2,c}}\right), -c_{2,c}W_0\left(-\frac{c_{2,bi}}{c_{2,c}}\mathrm{e}^{-c_{2,bi}/c_{2,c}}\right)\right) \tag{120}$$

and for $c_{2,\,bi} \geq c_{2,\,c}$ (cf. eq 95)

$$\left(-c_{2,c}W_0\left(-\frac{c_{2,bi}}{c_{2,c}}\mathrm{e}^{-c_{2,bi}/c_{2,c}}\right), -c_{2,c}W_{-1}\left(-\frac{c_{2,bi}}{c_{2,c}}\mathrm{e}^{-c_{2,bi}/c_{2,c}}\right), c_{\mathrm{tot}} - \left(-c_{2,c}W_0\left(-\frac{c_{2,bi}}{c_{2,c}}\mathrm{e}^{-c_{2,bi}/c_{2,c}}\right) - c_{2,c}W_{-1}\left(-\frac{c_{2,bi}}{c_{2,c}}\mathrm{e}^{-c_{2,bi}/c_{2,c}}\right)\right)\right) \tag{121}$$

This leads to the conditions for the intersection

$$c_{\mathrm{tot}} - \left(-c_{2,c}W_{-1}\left(-\frac{c_{2,bi}}{c_{2,c}}\mathrm{e}^{-c_{2,bi}/c_{2,c}}\right) - c_{2,c}W_0\left(-\frac{c_{2,bi}}{c_{2,c}}\mathrm{e}^{-c_{2,bi}/c_{2,c}}\right)\right) = -c_{2,c}W_0\left(-\frac{c_{2,bi}}{c_{2,c}}\mathrm{e}^{-c_{1,bi}/c_{1,c}}\right) \tag{122}$$

$$-c_{2,c}W_{-1}\left(-\frac{c_{2,bi}}{c_{2,c}}\mathrm{e}^{-c_{2,bi}/c_{2,c}}\right) = -c_{2,c}W_{-1}\left(-\frac{c_{2,bi}}{c_{2,c}}\mathrm{e}^{-c_{1,bi}/c_{1,c}}\right) \tag{123}$$

$$-c_{2,c}W_0\left(-\frac{c_{2,bi}}{c_{2,c}}\mathrm{e}^{-c_{2,bi}/c_{2,c}}\right) = c_{\mathrm{tot}} - \left(-c_{2,c}W_0\left(-\frac{c_{2,bi}}{c_{2,c}}\mathrm{e}^{-c_{2,bi}/c_{2,c}}\right) - c_{2,c}W_{-1}\left(-\frac{c_{2,bi}}{c_{2,c}}\mathrm{e}^{-c_{2,bi}/c_{2,c}}\right)\right) \tag{124}$$

Here, eq 123 is always true, and eqs 122 and 124 lead to the same expression.

$$c_{\mathrm{tot}} - c_{2,c}\left(-W_{-1}\left(-\frac{c_{2,bi}}{c_{2,c}}\mathrm{e}^{-c_{2,bi}/c_{2,c}}\right) - 2W_0\left(-\frac{c_{2,bi}}{c_{2,c}}\mathrm{e}^{-c_{2,bi}/c_{2,c}}\right)\right) = 0 \tag{125}$$

which is the same as $c_{\mathrm{tot}} = 2c^{\mathrm{I}}_{2,\,bi} + c^{\mathrm{II}}_{2,\,bi}$ or $c_{\mathrm{tot}} = c^{\mathrm{II}}_{1,\,bi} + c^{\mathrm{II}}_{2,\,bi} + c^{\mathrm{II}}_{3,\,bi}$ for the coordinates in the point where the binodals intersect. Figure 2d indicates that this is the requirement for the yellow triangle, if the phase with $c_{2,\,bi} \leq c_{2,\,c}$ is labeled I and $c_{2,\,bi} \geq c_{2,\,c}$ is labeled II.

Figure 8 shows the Helmholtz free energy $F/(RTV)$ along the bisector from one of its vertices to the center of the Gibbs triangle. It is observed that the curve for $c_{\mathrm{tot}} = 1.5$ mol/m^3 has a minimum in free energy, whereas the curve for $c_{\mathrm{tot}} = 1.25$ mol/m^3 is monotonically decreasing (and does not have a minimum, therefore). For $c_{\mathrm{tot}} = 1.3728...$ mol/m^3, a transition takes place between both cases.

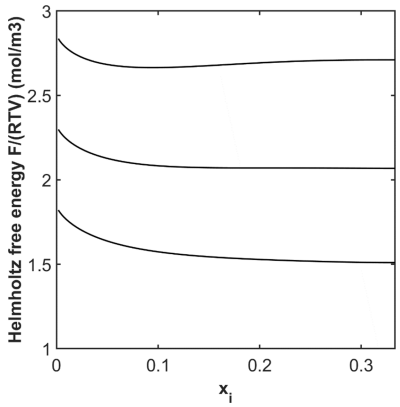

Figure 8. Normalized Helmholtz free energy $F/(RTV)$ as a function of the molar fracttion x_i for c_{tot}= 1.5, 1.3728..., 1.25 mol/m^3 (from top to bottom) following the bisector from one of its vertices to the center of the Gibbs triangle. Here B = 1 m^3/mol and$C$ = 2 m^3/mol.

(e) Point at the common top of the in-Gibbs-triangle binodals

The critical curve, eq 22, is a ringlike structure for symmetric mixtures, which typically has two intersections with a plane like $c_2 = c_3$. So for

$$(c_{1,c},\, c_{2,c},\, c_{3,c}) = \left(\frac{1}{2(C(S_{c,21} + S_{c,31}) - B)}, \frac{1}{2(CS_{c,12}(1 - S_{c,31}) - B)}, \frac{1}{2(CS_{c,13}(1 - S_{c,21}) - B)}\right) \tag{126}$$

The condition $c_{2,c} = c_{3,c}$ implies

$$\frac{1}{2(CS_{c,12}(1 - S_{c,31}) - B)} = \frac{1}{2(CS_{c,13}(1 - S_{c,21}) - B)} \tag{127}$$

or

https://doi.org/10.1021/acsomega.3c02604
ACS Omega 2023, 8, 28387−28408

$$S_{c,21}(1 - S_{c,21}) = S_{c,31}(1 - S_{c,31}) \tag{128}$$

There are two solutions

$$S_{c,21} = S_{c,31} \tag{129}$$

and

$$S_{c,21} = 1 - S_{c,31} \tag{130}$$

(or generally, $S_{c,21} + S_{c,31} = 1$). The solution related to eq 129 is out-of-Gibbs-triangle and will be discussed in Appendix A.5. Here, we will consider the situation associated with eq 130: it can be easily seen that substituting eq 130 into eq 126 leads to critical coordinates of $c_{1,c} = c_{2,c} = c_{3,c} = \frac{1}{2(C-B)}$.

A.5. Some Expressions for the Out-of-Gibbs-Triangle Binodals (Maximally Symmetric Mixture)

(a) Demonstration that the out-of-Gibbs-triangle binodals do not lay in the Gibbs triangle

The tangent plane to a critical point on the critical curve (eq 22) is

$$(c_1 - c_{1,c}) - \frac{1}{S_{c,21}}(c_2 - c_{2,c}) - \frac{1}{S_{c,31}}(c_3 - c_{3,c}) = 0 \tag{131}$$

The problem involves two planes (Gibbs triangle and the tangent plane), with normalized normal vectors

$$\boldsymbol{n}_{\text{Gibbs plane}} = \frac{1}{\sqrt{3}}\begin{pmatrix}1\\1\\1\end{pmatrix} \text{ and } \boldsymbol{n}_{\text{critical plane}} = \frac{1}{\sqrt{1 + \frac{1}{S_{c,21}^2} + \frac{1}{S_{c,31}^2}}}\begin{pmatrix}1\\ -\frac{1}{S_{c,21}}\\ -\frac{1}{S_{c,31}}\end{pmatrix} \tag{132}$$

Note that by definition, $S_{c,11} = -1$; so, the critical plane normal vector on the right can be written in a form in which all coordinates are treated equivalently.

We would like to calculate the (length of the) projection of the normal $\boldsymbol{n}_{\text{critical plane}}$ on the plane $c_1 + c_2 + c_3 = c_{\text{tot}}$ (i.e., the rejection of $\boldsymbol{n}_{\text{critical plane}}$ on $\boldsymbol{n}_{\text{Gibbs plane}}$). If the tangent plane is parallel to the Gibbs triangle, the length of the projection is 0. If the tangent plane is perpendicular to the Gibbs triangle, the length of the projection is 1, with the direction of the projection being perpendicular to the intersection of both planes. Any length smaller than unity suggests that the coexisting phases can be found "out of plane" above and below the Gibbs triangle.

The projection of $\boldsymbol{n}_{\text{critical plane}}$ on the plane with the normal vector $\boldsymbol{n}_{\text{Gibbs plane}}$ is given by (using that the normal vectors have been normalized)

$$\begin{aligned}
&\boldsymbol{n}_{\text{critical plane}} - (\boldsymbol{n}_{\text{critical plane}} \cdot \boldsymbol{n}_{c_{\text{tot}}\text{ plane}})\boldsymbol{n}_{\text{Gibbs plane}} \\
&= \frac{1}{\sqrt{1 + \frac{1}{S_{c,21}^2} + \frac{1}{S_{c,31}^2}}}\begin{pmatrix}1\\ -\frac{1}{S_{c,21}}\\ -\frac{1}{S_{c,31}}\end{pmatrix} \\
&\quad - \frac{1}{3\cdot\sqrt{1 + \frac{1}{S_{c,21}^2} + \frac{1}{S_{c,31}^2}}}\left(\begin{pmatrix}1\\ -\frac{1}{S_{c,21}}\\ -\frac{1}{S_{c,31}}\end{pmatrix}\cdot\begin{pmatrix}1\\1\\1\end{pmatrix}\right)\begin{pmatrix}1\\1\\1\end{pmatrix} \\
&= \frac{1}{3\cdot\sqrt{S_{c,21}^2 S_{c,31}^2 + S_{c,21}^2 + S_{c,31}^2}}\begin{pmatrix}2S_{c,21}S_{c,31} + S_{c,21} + S_{c,31}\\ -S_{c,21}S_{c,31} + S_{c,21} - 2S_{c,31}\\ -S_{c,21}S_{c,31} - 2S_{c,21} + S_{c,31}\end{pmatrix}
\end{aligned} \tag{133}$$

where the tangents in eq 133 should satisfy eq 23. The conclusion of this equation is that the projection of $\boldsymbol{n}_{\text{critical plane}}$ on the plane with the normal vector $\boldsymbol{n}_{c_{\text{tot}}\text{ plane}}$ does not always have the same length, and therefore, the critical plane does not always coincide with the c_{tot} (or Gibbs) plane. The projections are plotted in Figure 2a–f.

(b) Out-of-Gibbs-triangle binodal for $c_2 = c_3$

In Appendix A.4, we identified a solution to the critical coordinates in eq 126 for the condition $S_{c,21} = S_{c,31}$ (eq 129). In the following section, it will be shown that this solution leads to out-of-Gibbs-triangle binodals. Equation 23 can be written in the maximally symmetric case as

$$(2CS_{c,21} - B)^2 - 2S_{c,21}(C - (B + C)S_{c,21})^2 = 0 \tag{134}$$

or

$$S_{c,21}{}^3 - 2\frac{C(B + 2C)}{(B + C)^2}S_{c,21}{}^2 + \frac{C(2B + C)}{(B + C)^2}S_{c,21} - \frac{1}{2}\frac{B^2}{(B + C)^2} = 0 \tag{135}$$

For $B = 1$ and $C = 2$ m^3/mol, the relevant $S_{c,21}$ is $\{40 + 8\sqrt{46}\cos((\tan^{-1}(405\sqrt{191}/8267) + 2k\pi)/3)\}/54$

≈ 0.4197

for $k = 2$. The associated coordinates are $c_{1,c} = 0.7366$, $c_{2,c} = 0.2832$, and $c_{3,c} = 0.2832$ mol/m^3; so, the maximum of the critical curve can be found at $c_{\text{tot}} = 1.3031$ mol/m^3.

Under the assumption $c_2 = c_3$, i.e. associative phase separation between two of the components, we can write for eqs 51

https://doi.org/10.1021/acsomega.3c02604
ACS Omega 2023, 8, 28387−28408

$$\left(\frac{c_1^{\mathrm{I}}}{c_{1,s}}-1\right)-\left(\frac{c_1^{\mathrm{II}}}{c_{1,s}}-1\right) = -S_{m,12}\frac{c_{2,s}}{c_{1,s}}\left(\left(\frac{c_2^{\mathrm{I}}}{c_{2,s}}-1\right)-\left(\frac{c_2^{\mathrm{II}}}{c_{2,s}}-1\right)\right) \tag{136}$$

$$\left(\frac{c_2^{\mathrm{I}}}{c_{2,s}}-1\right)-\left(\frac{c_2^{\mathrm{II}}}{c_{2,s}}-1\right)=\left(\frac{c_2^{\mathrm{I}}}{c_{2,s}}-1\right)-\left(\frac{c_2^{\mathrm{II}}}{c_{2,s}}-1\right) \tag{137}$$

$$\left(\frac{c_2^{\mathrm{I}}}{c_{2,s}}-1\right)-\left(\frac{c_2^{\mathrm{II}}}{c_{2,s}}-1\right) = -S_{m,21}\frac{c_{1,s}}{c_{2,s}}\left(\left(\frac{c_1^{\mathrm{I}}}{c_{1,s}}-1\right)-\left(\frac{c_1^{\mathrm{II}}}{c_{1,s}}-1\right)\right) \tag{138}$$

Equation 137 is always true, and eqs 136 and 138 are identical and therefore the only equation that we need to use going forward in this derivation. Combined with eq 49, we have

$$\left(\frac{c_1^{\mathrm{I}}}{c_{1,s}}-1\right)+\left(\frac{c_1^{\mathrm{II}}}{c_{1,s}}-1\right) = 2S_{m,21}\left(\left(\frac{c_2^{\mathrm{I}}}{c_{2,s}}-1\right)+\left(\frac{c_2^{\mathrm{II}}}{c_{2,s}}-1\right)\right) \tag{139}$$

$$\left(\frac{c_1^{\mathrm{I}}}{c_{1,s}}-1\right)-\left(\frac{c_1^{\mathrm{II}}}{c_{1,s}}-1\right) = -\frac{1}{S_{m,21}}\frac{c_{2,s}}{c_{1,s}}\left(\left(\frac{c_2^{\mathrm{I}}}{c_{2,s}}-1\right)-\left(\frac{c_2^{\mathrm{II}}}{c_{2,s}}-1\right)\right) \tag{140}$$

By subtraction and addition, expressions can be obtained for $\left(\frac{c_1^{\mathrm{I}}}{c_{1,s}}-1\right)$ and $\left(\frac{c_2^{\mathrm{I}}}{c_{2,s}}-1\right)$, each in terms of $\left(\frac{c_1^{\mathrm{II}}}{c_{1,s}}-1\right)$ and $\left(\frac{c_2^{\mathrm{II}}}{c_{2,s}}-1\right)$. The result in matrix notation is

$$\begin{pmatrix}\left(\frac{c_1^{\mathrm{I}}}{c_{1,s}}-1\right)\\ \left(\frac{c_2^{\mathrm{I}}}{c_{2,s}}-1\right)\end{pmatrix} = \begin{pmatrix}\frac{\left(S_{m,21}\sqrt{\frac{2c_{1,s}}{c_{2,s}}}-\frac{1}{S_{m,21}}\sqrt{\frac{c_{2,s}}{2c_{1,s}}}\right)}{\left(S_{m,21}\sqrt{\frac{2c_{1,s}}{c_{2,s}}}+\frac{1}{S_{m,21}}\sqrt{\frac{c_{2,s}}{2c_{1,s}}}\right)} & \frac{4\sqrt{\frac{c_{2,s}}{2c_{1,s}}}}{\left(S_{m,21}\sqrt{\frac{2c_{1,s}}{c_{2,s}}}+\frac{1}{S_{m,21}}\sqrt{\frac{c_{2,s}}{2c_{1,s}}}\right)}\\ \frac{\sqrt{\frac{2c_{1,s}}{c_{2,s}}}}{\left(S_{m,21}\sqrt{\frac{2c_{1,s}}{c_{2,s}}}+\frac{1}{S_{m,21}}\sqrt{\frac{c_{2,s}}{2c_{1,s}}}\right)} & -\frac{\left(S_{m,21}\sqrt{\frac{2c_{1,s}}{c_{2,s}}}-\frac{1}{S_{m,21}}\sqrt{\frac{c_{2,s}}{2c_{1,s}}}\right)}{\left(S_{m,21}\sqrt{\frac{2c_{1,s}}{c_{2,s}}}+\frac{1}{S_{m,21}}\sqrt{\frac{c_{2,s}}{2c_{1,s}}}\right)}\end{pmatrix}\begin{pmatrix}\left(\frac{c_1^{\mathrm{II}}}{c_{1,s}}-1\right)\\ \left(\frac{c_2^{\mathrm{II}}}{c_{2,s}}-1\right)\end{pmatrix} \tag{141}$$

The tie-lines are not quite parallel, but $S_{m,21} \to S_{c,21}$ when the tie-lines are near the critical point.

A.6. Consistency Check for Coexisting Phases in Ternary Mixtures

In previous work on binary polymer mixtures, a consistency relation was obtained, which was formulated exclusively in terms of the concentrations of the coexisting phases but without any of the virial coefficients (eq 105 in ref 8. It was later shown that this relation can be obtained directly from the coexistence equation (eq 11. Here, the previous approach is applied to the coexistence equations for $N = 3$ and $P = 2$ (eqs 37−40), which can be rearranged as

$$\begin{aligned}&(c_1^{\mathrm{I}}-c_1^{\mathrm{II}})+(c_2^{\mathrm{I}}-c_2^{\mathrm{II}})+(c_3^{\mathrm{I}}-c_3^{\mathrm{II}})+B_{11}(c_1^{\mathrm{I}}+c_1^{\mathrm{II}})\\ &\quad(c_1^{\mathrm{I}}-c_1^{\mathrm{II}})+B_{22}(c_2^{\mathrm{I}}+c_2^{\mathrm{II}})(c_2^{\mathrm{I}}-c_2^{\mathrm{II}})\\ &\quad+B_{33}(c_3^{\mathrm{I}}+c_3^{\mathrm{II}})(c_3^{\mathrm{I}}-c_3^{\mathrm{II}})+2B_{12}(c_1^{\mathrm{I}}c_2^{\mathrm{I}}-c_1^{\mathrm{II}}c_2^{\mathrm{II}})\\ &\quad+2B_{13}(c_1^{\mathrm{I}}c_3^{\mathrm{I}}-c_1^{\mathrm{II}}c_3^{\mathrm{II}})+2B_{23}(c_2^{\mathrm{I}}c_3^{\mathrm{I}}-c_2^{\mathrm{II}}c_3^{\mathrm{II}})\\ &\quad=0\end{aligned} \tag{142}$$

$$\begin{aligned}2B_{11}(c_1^{\mathrm{I}}-c_1^{\mathrm{II}}) &= \ln\left(\frac{c_1^{\mathrm{II}}}{c_1^{\mathrm{I}}}\right)-2B_{12}(c_2^{\mathrm{I}}-c_2^{\mathrm{II}})\\ &\quad-2B_{13}(c_3^{\mathrm{I}}-c_3^{\mathrm{II}})\end{aligned} \tag{143}$$

$$\begin{aligned}2B_{22}(c_2^{\mathrm{I}}-c_2^{\mathrm{II}}) &= \ln\left(\frac{c_2^{\mathrm{II}}}{c_2^{\mathrm{I}}}\right)-2B_{12}(c_1^{\mathrm{I}}-c_1^{\mathrm{II}})\\ &\quad-2B_{23}(c_3^{\mathrm{I}}-c_3^{\mathrm{II}})\end{aligned} \tag{144}$$

$$\begin{aligned}2B_{33}(c_3^{\mathrm{I}}-c_3^{\mathrm{II}}) &= \ln\left(\frac{c_3^{\mathrm{II}}}{c_3^{\mathrm{I}}}\right)-2B_{13}(c_1^{\mathrm{I}}-c_1^{\mathrm{II}})\\ &\quad-2B_{23}(c_2^{\mathrm{I}}-c_2^{\mathrm{II}})\end{aligned} \tag{145}$$

Subsequently substituting eqs 143−145 into eq 142

$$\begin{aligned}&(c_1^{\mathrm{I}}-c_1^{\mathrm{II}})+(c_2^{\mathrm{I}}-c_2^{\mathrm{II}})+(c_3^{\mathrm{I}}-c_3^{\mathrm{II}})+\frac{1}{2}(c_1^{\mathrm{I}}+c_1^{\mathrm{II}})\\ &\quad\left(\ln\left(\frac{c_1^{\mathrm{II}}}{c_1^{\mathrm{I}}}\right)-2B_{12}(c_2^{\mathrm{I}}-c_2^{\mathrm{II}})-2B_{13}(c_3^{\mathrm{I}}-c_3^{\mathrm{II}})\right)\\ &\quad+\frac{1}{2}(c_2^{\mathrm{I}}+c_2^{\mathrm{II}})\left(\ln\left(\frac{c_2^{\mathrm{II}}}{c_2^{\mathrm{I}}}\right)-2B_{12}(c_1^{\mathrm{I}}-c_1^{\mathrm{II}})\right.\\ &\quad\left.-2B_{23}(c_3^{\mathrm{I}}-c_3^{\mathrm{II}})\right)+\frac{1}{2}(c_3^{\mathrm{I}}+c_3^{\mathrm{II}})\\ &\quad\left(\ln\left(\frac{c_3^{\mathrm{II}}}{c_3^{\mathrm{I}}}\right)-2B_{13}(c_1^{\mathrm{I}}-c_1^{\mathrm{II}})-2B_{23}(c_2^{\mathrm{I}}-c_2^{\mathrm{II}})\right)\\ &\quad+2B_{12}(c_1^{\mathrm{I}}c_2^{\mathrm{I}}-c_1^{\mathrm{II}}c_2^{\mathrm{II}})+2B_{13}(c_1^{\mathrm{I}}c_3^{\mathrm{I}}-c_1^{\mathrm{II}}c_3^{\mathrm{II}})\\ &\quad+2B_{23}(c_2^{\mathrm{I}}c_3^{\mathrm{I}}-c_2^{\mathrm{II}}c_3^{\mathrm{II}})\\ &\quad=0\end{aligned} \tag{146}$$

This can be simplified by canceling terms as

https://doi.org/10.1021/acsomega.3c02604
ACS Omega 2023, 8, 28387−28408

$$(c_1^{\mathrm{I}} - c_1^{\mathrm{II}}) + (c_2^{\mathrm{I}} - c_2^{\mathrm{II}}) + (c_3^{\mathrm{I}} - c_3^{\mathrm{II}}) + \frac{1}{2}(c_1^{\mathrm{I}} + c_1^{\mathrm{II}})\ln\left(\frac{c_1^{\mathrm{II}}}{c_1^{\mathrm{I}}}\right) + \frac{1}{2}(c_2^{\mathrm{I}} + c_2^{\mathrm{II}})\ln\left(\frac{c_2^{\mathrm{II}}}{c_2^{\mathrm{I}}}\right) + \frac{1}{2}(c_3^{\mathrm{I}} + c_3^{\mathrm{II}})\ln\left(\frac{c_3^{\mathrm{II}}}{c_3^{\mathrm{I}}}\right) = 0 \quad (147)$$

The same approach can be taken in the case of $N = 3$ and $P = 3$, which yields an additional equivalent relation linking the concentrations in phases I and III. Combining this additional equation with eq 146 links the concentrations in phases II and III in a similar way.

■ ASSOCIATED CONTENT

Supporting Information

The Supporting Information is available free of charge at https://pubs.acs.org/doi/10.1021/acsomega.3c02604.

Video for the ternary phase diagrams as a function of c_{tot} (MP4)

Ternary phase diagrams as a function of c_{tot} for the symmetric mixture (PDF)

■ AUTHOR INFORMATION

Corresponding Author

Paul Venema − *Laboratory of Physics and Physical Chemistry of Foods, Department of Agrotechnology and Food Sciences, Wageningen University and Research, NL-6708 WG Wageningen, The Netherlands*; Email: paul.venema@wur.nl

Author

Arjen Bot − *Laboratory of Physics and Physical Chemistry of Foods, Department of Agrotechnology and Food Sciences, Wageningen University and Research, NL-6708 WG Wageningen, The Netherlands; Unilever Foods Innovation Centre, NL-6708 WH Wageningen, The Netherlands;* orcid.org/0000-0002-2065-8964

Complete contact information is available at: https://pubs.acs.org/10.1021/acsomega.3c02604

Notes

The authors declare no competing financial interest.

■ REFERENCES

(1) Albertsson, P.A. *Partition of cell particles and macromolecules*; 3rd edition, Wiley: New York, 1986.

(2) Choi, J. M.; Holehouse, A. S.; Pappu, R. V. Physical principles underlying the complex biology of intracellular phase transitions. *Annu. Rev. Biophys.* **2020**, *49*, 107−133.

(3) Mace, C. R.; Akbulut, O.; Kumar, A. A.; Shapiro, N. D.; Derda, R.; Patton, M. R.; Whitesides, G. M. Aqueous multiphase systems of polymers and surfactants provide self-assembling step-gradients in density. *J. Am. Chem. Soc.* **2012**, *134*, 9094−9097.

(4) van der Bruggen, B.; Vandecasteele, C.; van Gestel, T.; Doyen, W.; Leysen, R. A review of pressure-driven membrane processes in wastewater treatment and drinking water production. *Environ. Prog.* **2003**, *22*, 46−56.

(5) Bot, A.; Foster, T. J.; Lundin, L. Modelling acidified emulsion gels as Matryoshka composites: Firmness and syneresis. *Food Hydrocolloids* **2014**, *34*, 88−97.

(6) Hyman, A. A.; Weber, C. A.; Jülicher, F. Liquid-liquid phase separation in biology. *Annu. Rev. Cell Dev. Biol.* **2014**, *30*, 39−58.

(7) Ersch, C.; van der Linden, E.; Martin, A.; Venema, P. Interactions in protein mixtures. Part II: A virial approach to predict phase behavior. *Food Hydrocolloids* **2016**, *52*, 991−1002.

(8) Dewi, B. P. C.; van der Linden, E.; Bot, A.; Venema, P. Second order virial coefficients from phase diagrams. *Food Hydrocolloids* **2020**, *101*, No. 105546.

(9) Dewi, B. P. C.; van der Linden, E.; Bot, A.; Venema, P. Corrigendum to "second order virial coefficients from phase diagrams." [Food Hydrocolloids 101 (2020) 105546]. *Food Hydrocolloids* **2021**, *112*, No. 106324.

(10) Bot, A.; Dewi, B. P. C.; Venema, P. Phase-separating binary polymer mixtures: the degeneracy of the virial coefficients and their extraction from phase diagrams. *ACS Omega* **2021**, *6*, 7862−7878.

(11) Bot, A.; Dewi, B. P. C.; Venema, P. Addition to "Phase-separating binary polymer mixtures: the degeneracy of the virial coefficients and their extraction from phase diagrams.". *ACS Omega* **2021**, *6*, 20086−20087.

(12) Edmond, E.; Ogston, A. G. An approach to the study of phase separation in ternary aqueous systems. *Biochem. J.* **1968**, *109*, 569−576.

(13) Bot, A.; Dewi, B. P. C.; Kool, T.; van der Linden, E.; Venema, P. Meta-analysis of critical points to determine second virial coefficients for binary biopolymer mixtures. *Food Hydrocolloids* **2022**, *126*, No. 107473.

(14) Edmond, E.; Ogston, A. G. Phase separation in an aqueous quaternary system. *Biochem. J.* **1970**, *117*, 85−89.

(15) Huang, C.; Olvera de la Cruz, M.; Swift, B. W. Phase separation of ternary mixtures: Symmetric polymer blends. *Macromolecules* **1995**, *28*, 7996−8005.

(16) Zhou, J.; van Duijneveldt, J. S.; Vincent, B. Two-stage phase separation in ternary colloid−polymer mixtures. *Phys. Chem. Chem. Phys.* **2011**, *13*, 110−113.

(17) Mao, S.; Kuldinow, D.; Haataja, M. P.; Košmrlj, A. Phase behavior and morphology of multicomponent liquid mixtures. *Soft Matter* **2019**, *15*, 1297−1311.

(18) Warren, P. B. Phase behavior of a colloid + binary polymer mixture: Theory. *Langmuir* **1997**, *13*, 4588−4594.

(19) Sear, R. P.; Frenkel, D. Phase behavior of colloid plus polydisperse polymer mixtures. *Phys. Rev. E* **1997**, *55*, 1677−1681.

(20) Sollich, P. Predicting phase equilibria in polydisperse systems. *J. Phys.: Condens. Matter* **2002**, *14*, R79.

(21) Edelman, M. W.; van der Linden, E.; Tromp, R. H. Phase separation of aqueous mixtures of poly(ethylene oxide) and dextran. *Macromolecules* **2003**, *36*, 7783−7790.

(22) Sturtewagen, L.; van der Linden, E. Effects of polydispersity on the phase behavior of additive hard spheres in solution. *Molecules* **2021**, *26*, 1543.

(23) Sturtewagen, L.; van der Linden, E. Towards predicting partitioning of enzymes between macromolecular phases: Effects of polydispersity on the phase behavior of nonadditive hard spheres in solution. *Molecules* **2022**, *27*, 6354.

(24) McMillan, W. G., Jr.; Mayer, J. E. The Statistical Thermodynamics of Multicomponent Systems. *J. Chem. Phys.* **1945**, *13*, 276−305.

(25) Solokhin, M. A.; Solokhin, A. V.; Timofeev, V. S. Phase-equilibrium stability criterion in terms of the eigenvalues of the Hessian matrix of the Gibbs potential. *Theor. Found. Chem. Eng.* **2002**, *36*, 444−446.

(26) Gibbs, J. W. On the equilibrium of heterogeneous substances. *Trans. Conn. Acad.* **1874-1878**, *III*, 108−248.

(27) Reid, R. C.; Beegle, B. L. Critical point criteria in Legendre transform notation. *AIChE J.* **1977**, *23*, 726−732.

(28) Beegle, B. L.; Modell, M.; Reid, R. C. Legendre transforms and their application in thermodynamics. *AIChE J.* **1974**, *20*, 1194−1200.

(29) Beegle, B. L.; Modell, M.; Reid, R. C. Thermodynamic stability criterion for pure substances and mixtures. *AIChE J.* **1974**, *20*, 1200−1206.

(30) Kipnis, A.Y.; Yavelov, B.E.; Rowlinson, J.S. *Van der Waals and molecular science*; Oxford University Press, 2001, p.256. Lectures

notes by van der Waals as edited by Kohnstamm include the following statement: "*It is not easy to determine analytically the boundary between [absolute] stable and metastable states, since whether a point lies in one region or the other depends on the peculiarities of the [free energy] surface, not only at the point under consideration, but also at other points far removed from it.*"

(31) Grinberg, V. Y.; Tolstoguzov, V. B. Thermodynamic incompatibility of proteins and polysaccharides in solutions. *Food Hydrocolloids* **1997**, *11*, 145−158.

(32) Corless, R. M.; Gonnet, G. H.; Hare, D. E. G.; Jeffrey, D. J.; Knuth, D. E. On the Lambert-W function. *Adv. Comput. Math.* **1996**, *5*, 329−359.

(33) West, D.R.F. *Ternary phase diagrams in materials science*; (3rd ed.) CRC Press, 2013, https://doi.org/10.1201/9781003077213

(34) Heidemann, R. A. The criteria for thermodynamic stability. *AIChE J.* **1975**, *21*, 824−826.

(35) Beegle, B.; Modell, M.; Reid, R. C. Reply. *AIChE J.* **1975**, *21*, 826.

(36) Bloustine, J.; Virmani, T.; Thurston, G. M.; Fraden, S. Light scattering and phase behavior of lysozyme-poly(ethylene glycol) mixtures. *Phys. Rev. Lett.* **2006**, *96*, No. 087803.

https://doi.org/10.1021/acsomega.3c02604
ACS Omega 2023, 8, 28387−28408